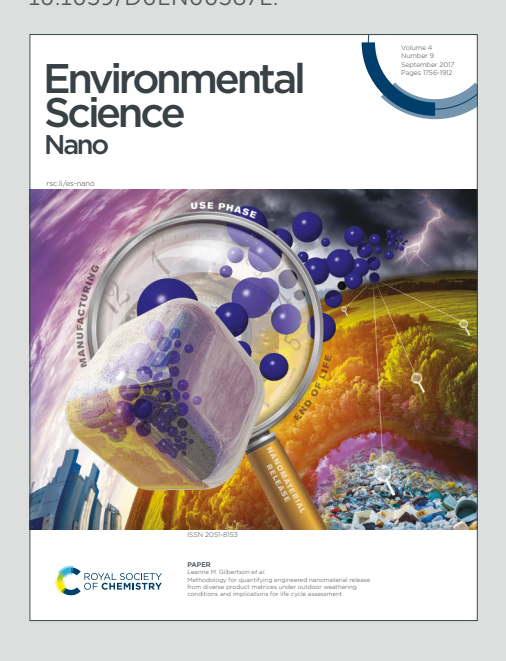
Check for updates

Environmental Science Nano



Accepted Manuscript

This article can be cited before page numbers have been issued, to do this please use: J. An, P. Hu, F. Li, H. Wu, Y. Shen, J. White, X. Tian, Z. Li and J. P. Giraldo, *Environ. Sci.: Nano*, 2020, DOI: 10.1039/D0EN00387E.



This is an Accepted Manuscript, which has been through the Royal Society of Chemistry peer review process and has been accepted for publication.

Accepted Manuscripts are published online shortly after acceptance, before technical editing, formatting and proof reading. Using this free service, authors can make their results available to the community, in citable form, before we publish the edited article. We will replace this Accepted Manuscript with the edited and formatted Advance Article as soon as it is available.

You can find more information about Accepted Manuscripts in the <u>Information for Authors</u>.

Please note that technical editing may introduce minor changes to the text and/or graphics, which may alter content. The journal's standard <u>Terms & Conditions</u> and the <u>Ethical guidelines</u> still apply. In no event shall the Royal Society of Chemistry be held responsible for any errors or omissions in this Accepted Manuscript or any consequences arising from the use of any information it contains.



View Article Online

DOI: 10.1039/D0EN00387E

Environmental significance

Seed priming with nanomaterials provides a sustainable and scalable tool to improve plant stress tolerance during the vulnerable seedling stage. We utilized molecular, physiological, and biochemical analytical tools to understand how priming seeds with cerium oxide nanoparticles (nanoceria) modifies seedling development under salinity stress. Soil salinity is a major environmental stress affecting plant agricultural production worldwide. Furthermore, nanoceria are important unintentionally released nanomaterials in the environment. The nanoparticles localized in seed tissues but not in seedlings, indicating that improvement in seedling root development under salinity stress is the result of genetic modifications. Nanoceria seed priming resulted in differentially expressed genes associated with ROS and Ca²⁺ conserved signaling pathways, suggesting unifying mechanisms of nanoparticle seed priming effects on plant stress tolerance.

Jing An^{a,b}, Peiguang Hu^b, Fangjun Li^a, Honghong Wu^{b□}, Yu Shen^{c,d}, Jason C. White^d, Xiaoli Tian^a, Zhaohu Li^{a*}, Juan Pablo Giraldo^{b*}

^a State Key Laboratory of Plant Physiology and Biochemistry, College of Agronomy and Biotechnology, China Agricultural University, Beijing 100193, China

^b Department of Botany and Plant Sciences, University of California, Riverside, California 92521, USA

^c Center for Sustainable Nanotechnology, Chemistry Department, University of Wisconsin, Wisconsin 53706, USA

^d Center for Sustainable Nanotechnology, Connecticut Agricultural Experimental Station, New Haven, Connecticut 06504, USA

□ Current address: College of Plant Science & Technology, Huazhong Agricultural
University, Wuhan 430070, China

*Corresponding author:

2

7 8

38 39

40 41

48 49 50

51 52

59 60 Juan Pablo Giraldo: <u>juanpablo.giraldo@ucr.edu</u>

Zhaohu Li: <u>lizhaohu@cau.edu.cn</u>

4 5 6

7 8

14:46.PM6 1 0

1:80202/52/9 or or osipwall 1:80203/3/2/9 or osipwall 2:803/3/2/9 or osipwall 2:803/3/2/9 or osipwall 3:803/3/2/9 or osipwall 3:803/3/9 or osipwall 3:

*⊉*6

2020 Day 2020 Burles of Suppose o

38

39 40

41 42 43

44 45

46 47

48 49

50 51 52

59 60

Abstract

Engineered nanomaterials interfaced with plant seeds can improve stress tolerance during the vulnerable seedling stage. Herein, we investigated how priming seeds with antioxidant poly (acrylic acid)-coated cerium oxide nanoparticles (PNC) impacts cotton (Gossypium hirsutum L.) seedling morphological, physiological, biochemical, and transcriptomic traits under salinity stress. Seeds primed with 500 mg/L PNC in water (24 h) and germinated under salinity stress (200 mM NaCl) retained nanoparticles in the seed coat inner tegmen, cotyledon, and root apical meristem. Seed priming with PNC significantly (P < 0.05) increased seedling root length (56%), fresh weight (41%), and dry weight (38%), modified root anatomical structure, and increased root vitality (114%) under salt stress compared with controls (water). PNC seed priming lead to a decrease in reactive oxygen species (ROS) accumulation in seedling roots (46%) and alleviated root morphological and physiological changes induced by salinity stress. Roots from exposed seeds exhibited similar Na content, significantly decreased K (6%), greater Ca (22%) and Mg content (60%) compared to controls. A total of 4,779 root transcripts were differentially expressed by PNC seed priming alone relative to controls with no nanoparticles under non-saline conditions. Under salinity stress, differentially expressed genes (DEGs) in PNC seed priming treatments relative to non-nanoparticle controls were associated with ROS pathways (13) and ion homeostasis (10), indicating that ROS and conserved Ca²⁺ plant signaling pathways likely play pivotal roles in PNC-induced improvement of salinity tolerance. These results provide potential unifying molecular mechanisms of nanoparticle-seed priming enhancement of plant salinity tolerance.

4 5 6

7

8

38 39 40

41 42

43 44

45 46 47

48 49

50 51

59 60 Nanomaterial, salt stress, seed priming, transcriptomic analysis, ion content, ROS.

1 Introduction

The pre-exposure or priming of seeds and seedlings to chemical agents (e.g. H₂O₂, ABA, NO, SA, etc.) or to abiotic stressors (such as salinity, drought, cold, etc.) is an effective and scalable technique to enable rapid and uniform seed germination, high seedling vigor, and improved yield in field crops under stress. 1-5 For example, seed priming with H₂O₂ improves tolerance to both salinity and drought stress by enabling plants to recognize and decode early signals that are rapidly activated when plants are subsequently exposed to stress.⁶ Seed priming with acetylsalicylic acid enhances the activities of antioxidant enzymes (catalase CAT, peroxidase POD, and superoxide dismutase SOD by 12-28%), thus reducing oxidative stress in treated seedlings. Nanoenabled agriculture is emerging as a novel approach to augment conventional crop production systems, allowing for the controlled release of agrochemicals (e.g. fertilizers, pesticides), targeted delivery of biomolecules (e.g., nucleotides, proteins, and activators) and monitoring plant health (e.g. sensors).8-10 Recent studies have demonstrated that interfacing plant seeds with nanomaterials result in positive effects on seedling development. 11 This approach has the advantage of minimizing nanoparticle exposure in the environment by priming seeds in contained facilities, with subsequent transfer to the field. However, there is little understanding of the molecular mechanisms underlying

4 5

6

7 8

38

39 40

41 42 43

44 45

46 47

48 49 50

51 52

53 54

59 60 the physiological and biochemical changes associated with nanoparticle treatment of seeds.

Cerium oxide nanoparticles (nanoceria, CeO₂-NPs) are widely used in the production of catalysts, sunscreens, fuel additives, microelectronics, and polishing agents, 12,13 thus constituting an important nanomaterial released into the environment. 14-16 Nanoscale CeO₂-NPs has Ce³⁺ and Ce⁴⁺ dangling bonds on the surface that enable antioxidant enzyme-mimetic activity through catalytic scavenging of reactive oxygen species (ROS). 17,18 CeO₂-NPs (10.3 nm, -16.9 mV, 50 mg/L) coated in a biocompatible polymer (poly (acrylic acid)) have demonstrated potential to protect Arabidopsis thaliana from oxidative stress by increasing photosystem II quantum yield (19%), carbon assimilation rates (67%), rubisco carboxylation rates (61%), and improving shoot biomass (18%). 19-²¹ Tumburu et al. demonstrated that long term exposure to uncoated CeO₂-NPs (23.3 nm, +35.9 mV, 500 mg/L, 12 days) increases Arabidopsis seed germination (42%), hypocotyl and cotyledon growth (61.5%), by altering the regulation of genes involved in stress responses, photosystems, cell wall proteins, and water and ion transport processes.²² In contrast, Andersen et al.¹⁴ reported that uncoated CeO₂-NPs (23.3 nm, zeta potential of +38 to 44 mV, 250-1000 mg/L) do not significantly alter germination in 10 crop species including cabbage (Brassica oleracea), carrot (Daucus carota), corn (Zea mays), cucumber (Cucumis sativus), lettuce (Lactuca sativa), oats (Avena sativa), onion (Allium cepa), ryegrass (Lolium perenne), soybean (Glycine max), and tomato (Lycopersicon lycopersicum), but impact root length in onion and ryegrass, lettuce, tomato, and cotyledon development cucumber. 14 Recently Zhang et al. 23 observed that

uncoated CeO₂-NPs (194.8 nm, +20.2 mV, 3 mg per plant) do not affect plant phenotype but induce marked down-regulation of a number of amino acids (threonine, tryptophan, L-cysteine, methionine, cycloleucine, aspartic acid, asparagine, tyrosine, and glutamic acid), and decreased Ca (32%) in roots of spinach plants (*Spinacia oleracea*). However, these previous studies do not explore the underlying molecular mechanisms of how seed priming with cerium oxide nanoparticles impact seedling development.

Soil salinity is a major abiotic stress affecting plant agricultural production worldwide. Approximately 20% of the world's cultivated lands and more than half of all irrigated lands are affected by salinity.²⁴ A high concentration of NaCl in soil reduces water potential and makes it more difficult for roots to extract water, causes an imbalance in cellular ions resulting in toxicity, osmotic stress and accumulation of ROS, which subsequently affects plant growth, morphology, and survival. 24,25 Rossi et al.26 reported that canola (Brassica napus L.) treated with polyvinylpyrrolidone (PVP) coated CeO₂ NPs (55.6 nm, -51.8 mV, 200, 1000 mg/L) had higher plant biomass and exhibited greater photosynthetic efficiency in both fresh and saline water irrigation conditions. The CeO₂-NPs improved physiological performance of canola under salinity stress by shortening the root apoplastic barriers, thereby allowing more Na⁺ transport to shoots and less accumulation of Na⁺ in the roots.²⁷ Similarly, uncoated CeO₂-NPs (620.7 nm, -11.6 mV, 500 mg/L) were reported to significantly alleviate the DNA damage in NaCl treated rice.²⁸ CeO₂-NPs (10.3 nm, -16.9 mV, 50 mg/L) coated with poly (acrylic acid) also improved Arabidopsis salinity stress tolerance by reducing leaf ROS levels

4 5

6

7 8

38

39 40 41

42 43

44 45

46 47

59 60 (hydroxyl radical 41% and hydrogen peroxide 44%), and increasing by one fold potassium in the leaf mesophyll.²¹

Cotton (Gossypium hirsutum L.) is an economically important crop and has been described as moderately salt-tolerant.^{25,29,30} Cotton seed germination and seedling development are affected by salinity.³¹ Seed germination and early seedling development are critical developmental stages for successful establishment of plants in the field and the most sensitive stages to environmental stresses.³² Therefore it is critical to enable novel approaches to improve cotton salinity tolerance during germination stage. Herein, we utilized molecular, physiological, and biochemical analytical tools to understand how priming seeds with CeO₂-NPs coated with poly (acrylic acid) (PNC) modify seedling development under salinity stress. Specifically, we assessed the impact of PNC priming of cotton seeds germinated under salt stress conditions (200 mM NaCl) on: 1) the location of PNC in seed tissues; 2) seedling germination, growth, anatomical structure and vitality; 3) ROS levels; 4) homeostasis of key elements involved in plant physiological responses (Na, K, Ca, and Mg); and 5) transcriptome profiles of ion homeostasis and metabolic pathways of ROS associated with salinity tolerance. This study elucidates how changes induced by PNC seed priming on seedling growth and anatomy are associated with cross talk of genes involved in conserved ion homeostasis and ROS enzymatic pathways (Figure 1).

14:46.PM6 1 0

1:8 0202/2020 or or osipeW 2 3 4 5 6 7 8

*⊉*6

2.1 Synthesis and characterization of cerium oxide nanoparticles

The PAA (poly (acrylic acid), M.W. 1800, Sigma Aldrich) functionalized cerium oxide nanoparticles (PNC) were synthesized as follows. The 0.217 g of Ce(NO₃)₃•6H₂O [cerium (III) nitric, 99%, Sigma Aldrich] in 0.5 mL of DI water and 0.450 g of PAA in 0.5 mL of DI water were added dropwise into 3 mL of NH₃•H₂O (ammonium hydroxide solution, 30%, Sigma Aldrich) while stirring at 650 rpm at ambient temperature. The mixture was stirred for 24 h, then purified with centrifugation filters (Amicon cell, MWCO 10k, Millipore Inc.) at 4500 rpm for 5 cycles to remove unreacted residuals. The final product, PNC, was stored at 4 °C until further use.

UV/Vis absorbance spectra were collected using a Shimadzu UV-2600 spectrophotometer. Dynamic light scattering (DLS) measurements were performed in DI water (pH 8.0) using a Malvern Zetasizer Nano S at the same concentration applied in seed priming experiments (500 mg/L). Transmission electron microscopy (TEM) was performed with a Philips FEI Tecnai 12 microscope operated at an accelerating voltage of 120 kV. The TEM samples were prepared by placing a drop of PNC in DI water (0.1 mg/mL) onto a Cu grid (400 mesh, Ted Pella) and then drying in air. The zeta potential of PNC was measured in DI water (pH 8.0) with a Malvern Zetasizer Nano ZS. The X-ray photoelectron spectroscopy (XPS) was carried out with a Kratos AXIS ULTRADLD XPS system equipped with an Al Kα monochromated X-ray source and a 165-mm mean radius electron energy hemispherical analyzer. The spectra were aligned using C1s (284.8 eV) as a reference. The experimental data were curve fitted into several

 components of Gaussian-Lorentzian peaks with Shirley background using the CasaXPS program (version 2.3.16). The Ce 3d peaks have described the structures u''', u'', u', u, u₀, v''', v', v, and v₀. $^{33-35}$ Peak areas (*A*) of Ce³⁺ and Ce⁴⁺ components are commonly used to estimate their relative concentrations (*C*) using the following equations^{35,36}:

$$A_{Ce^{3+}} = A_{u'} + A_{v'} + A_{u_0} + A_{v_0}$$
 (1)

$$A_{Ce^{4+}} = A_{u'''} + A_{v'''} + A_{u''} + A_{v''} + A_{u} + A_{v}$$
 (2)

$$C_{Ce^{3}} = \frac{A_{Ce^{3}}}{A_{Ce^{3}} + A_{Ce^{4}}}$$
(3)

2.2 Plant material, stress treatments, and growth conditions

Cotton (*Gossypium hirsutum* L., cultivar Acala 1517-08) acid-delinted seeds were sterilized with 70% ethanol for 1 min and washed with DI water for five times. The sterilized seeds were transferred to either 0 or 500 mg/L of PNC in DI water for 24 h of priming. After PNC priming, the seeds were wiped with filter paper and rolled between two layers of germination paper (Anchor Paper Co., Saint Paul, MN, USA). Moistened germination paper with 200 mM NaCl or DI water were used as the salinity stress treatment or the NaCl-free control, respectively. Seeds in the germination paper were placed in plastic self-sealing bags and were allowed to germinate in a growth chamber (Adaptis 1000, Conviron) at 25/22 °C (day/night) with a 14/10 h day and night photoperiod. Seed germination was determined when the radicle was longer than 5 mm.

 To visualize PNC in the cotton seeds, the nanoparticles were labeled with 1,1'dioctadecyl-3,3,3',3'-tetramethylindocarbocyanine perchlorate (Dil, Thermo Fisher
Scientific) fluorescent dye as reported previously.³⁷ Briefly, 0.2 mL of Dil solution (0.3 mg/mL) in dimethyl sulfoxide (DMSO, 99.9%, Fisher) was added dropwise into 4.0 mL
of PNC in DI water (1.5 mg/mL) while stirring at 1000 rpm at room temperature
overnight. The mixture was purified with centrifugation filters (Amicon cell, MWCO 10k,
Millipore Inc.) at 4500 rpm for 5 times to remove free Dil. The final product, Dil-PNC,
was stored at 4 °C until further use.

Sterilized cotton seeds were soaked with Dil-PNC in DI water (500 mg/L) for 24 h, and wiped with filter paper. The cotton seeds were dissected into seed coat inner tegmen, cotyledon and radicle. The tissue sections were mounted on microscope slides (Corning 2948-75×25) in a Carolina observation gel chamber (~1 mm thickness), filled with perfluorodecalin (PFD, 90%, Acros), and sealed with a coverslip (VWR). Images were captured using a Leica TCS-SP5 confocal microscope (Leica Microsystems, Wetzlar, Germany). Confocal microscopy imaging settings were: 40× water objective (HC PL APO 40x/1.10 W CORR CS2); laser excitation 514 nm, emission PMT 550-615 nm. At least 4 replicates were visualized for each treatment.

2.4 Plant growth and anatomy

Tisology Also Associated the second of the s

*⊉*6

 The germination rate was recorded every day after salinity stress. The length of roots and hypocotyls were measured 7d after salinity stress using a measuring scale. The cotton seedlings were separated into cotyledon, hypocotyl, and root to record fresh weights, followed by drying of the samples at 80 °C in an oven for 72 h to measure dry weights.

To determine root anatomical changes in seedlings grown under salinity stress, cross sections were taken at a distance of 1-1.5 cm from the apex of seedlings under salinity stress for 3d. The root segments were embedded in 7% agarose and sectioned into slices with 100 µm in thickness by using an oscillating tissue slicer (EMS 500, Electron Microscopy Sciences Inc., and Hatfield, PA). Samples were stained with 0.01% Toluidine Blue O for 1 min, and were washed gently with distilled water.³⁸ At least four biological replicates were used for each treatment. Images were visualized by a microscope (BZ-X710, Keyence, Osaka, Japan). The tissue total root area, area of the vascular cylinder, and area of xylem elements were analyzed with ImageJ.

2.5 Root vitality

Root vitality was determined using 2, 3, 5-triphenyltetrazolium chloride (TTC) following previously described methods with modification.^{39,40} Cotton root tips (~3 cm) were excised from salinity stressed (3d) seedlings and were submerged in 2 mL of 0.6% (w/v) TTC solution in sodium phosphate buffer (50 mM, pH 7.5). The samples were incubated for 1.5 h at ambient temperature, then washed with sodium phosphate buffer (50 mM,

pH 7.5) three times. Pictures of roots were taken with a Nikon Coolpix S7000 camera. ImageJ was used to quantify the root area and TTC color intensity.

2.6 Root ROS levels

ROS levels were assesed by histochemical staining methods using 3, 3'diaminobenzidine (DAB),41,42 and the fluorescent probe 2', 7'-dichlorodihydrofluorescein diacetate (H₂DCFDA, Thermo Fisher Scientific)^{20,21,43} after 3d of salinity stress. DAB is oxidized by hydrogen peroxide in the presence of heme-containing proteins, such as peroxidases, generating a dark brown precipitate. 6,41,42 For DAB staining, root tips (~3 cm) from each treatment were immersed in 0.5 mg/mL DAB in sodium phosphate buffer (50 mM, pH 7.5) overnight at ambient temperature in darkness. Pictures were taken with a Nikon Coolpix S7000 camera. ImageJ was used to quantify the root tip area and DAB color intensity. For H₂DCFDA experiments, root tips (~2 cm) were washed with sodium phosphate buffer (50 mM, pH 7.5) three times, then incubated with 25 µM H₂DCFDA in sodium phosphate buffer (50 mM, pH 7.5) for 30 min at ambient temperature in the dark. After washing with sodium phosphate buffer three times (50 mM, pH 7.5), the root samples (1-1.5 cm to root tip) were mounted on microscope slides in a Carolina observation gel (~2 mm) chamber, filled with PFD, and sealed with a coverslip. Roots were visualized and images were captured using Leica TCS-SP5 confocal microscope (Leica Microsystems, Wetzlar, Germany). Confocal microscopy imaging settings were: 10× objective (HCX PL APO 10x/0.40 CS); laser excitation 496 nm (30%) and 514 nm (10%), PMT 500-600 nm. Dye fluorescent intensity and root area were quantified by ImageJ.

14:46.PM6 1 0

1:8 0202/2020 or or osipeW 2 3 4 5 6 7 8

*⊉*6

2020 Day 2020 Burles of Suppose o

2.7 Plant tissue elemental analysis

Cotyledon, hypocotyl and root tissues from seedlings exposed to salinity stress (7d) were analyzed for elemental composition as described previously. 44–46 Dry tissues were macerated in a mortar and pestle. The samples (0.1 g) were then added to 50 mL polypropylene digestion tubes with 5 mL of concentrated nitric acid and heated at 115 °C for 45 min using a hot block (DigiPREP System; SCP science, Champlain, NY). After dilution, the content of Na, K, Ca, and Mg were quantified using inductively coupled plasma optical emission spectroscopy (ICP-OES) on an iCAP 6500 (Thermo Fisher Scientific, Waltham, MA). Individual element concentrations were calculated as mg/g (tissue dry mass).

2.8 RNA extraction, cDNA library construction, and RNA-seq

Root samples from seedlings under salinity stress (200 mM NaCl) and controls were harvested at different time points (0, 12, 24 and 48 h) defined as follows. W0: after H₂O priming and before salinity stress; P0: after PNC priming and before salinity stress; W12, W24, W48: after H₂O priming and grown under normal conditions for 12, 24 and 48 h, respectively; P12, P24, P48: after PNC priming and grown under normal conditions for 12, 24 and 48 h, respectively; WS12, WS24, WS48: after H₂O priming and grown under salinity stress for 12, 24 and 48 h, respectively; PS12, PS24, PS48: after PNC priming and grown under salinity stress for 12, 24 and 48 h, respectively. Three biological replicates from each treatment were used for RNA-Seq experiments, and each replicate

contained RNA materials collected from 15 seedlings and mixed to minimize the effect of transcriptome unevenness among plants. The samples were frozen in liquid nitrogen and stored at -80 °C for further use. RNA was extracted from root samples according to the PureLinkTM RNA Mini Kit (Invitrogen, CA, USA) protocol. The RNA was digested with PureLink DNase (Invitrogen, CA, USA) and purified by RNeasy Mini Kit (Qiagen, CA, USA). The RNA quality was measured by Nanodrop and Agilent 2100. The mRNAs were purified using Oligo (dT) beads, fragmented into small pieces, and then primed with random hexamers to synthesize the first-strand cDNA and second-strand cDNAs. After purification with AMPure XP beads, a cDNA library was established from PCR amplification of the fragments of double-strand cDNA. Finally, 42 cDNA libraries were sequenced on Illumina HiseqTM2500/4000 (Illumina, San Diego, CA, USA) at Beijing Allwegene Technology Co., Ltd (Beijing, China).

2.9 Identification of differential expression genes (DEGs)

Clean reads were aligned to the cotton genome (*Gossypium hirsutum*, nbi-AD1_genome_v1.1)⁴⁷ using STAR (version v2.5.2b) software after removing low quality reads such as adapter contamination, unknown nucleotides > 10%, or Q20 (percentage of sequences with sequencing error rates < 1%) > 50%. Gene expression levels in each library were normalized to fragments per kilobase of exon model per million mapped reads (FPKM). Using three biological replications, a gene was considered as a differentially expressed gene (DEGs) between the control and treatment if its log_2 fold change (FPKM_{PNC}/FPKM_{H2O})| \geq 1 and *P*-value adjusted for multiple testing (*Padj*-value)

*⊉*6

 < 0.05 analyzed by DEseq software (version 1.10.1). The heat map of PNC-regulated genes with or without salinity treatment was generated by log₁₀(FPKM + 0.001).

2.10 Statistical analysis

Data was compared with independent samples using a one-way ANOVA based on Duncan's test (two tailed) or Kruskal Wallis test in SPSS 20.0 software (IBM, New York, USA). Different lowercase letters indicate significant differences (*P* < 0.05).

3 Results and Discussion

3.1 Nanoceria characterization

Transmission electron microscopy (TEM) images illustrate an average PNC core size of 1.8 ± 0.3 nm (Figure 2B). The hydrodynamic diameter of the nanoparticles measured by dynamic light scattering was 2.1 ± 1.4 nm (Figure 2A) and the average zeta potential of PNC measured in DI water (pH 8.0) was -51.7 ± 11.5 (Figure 2C), indicating high negatively charged nanoparticles with size much smaller than reported plant cell wall pore size.⁴⁸ The XPS spectra indicated the existence of both Ce³⁺ and Ce⁴⁺ in PNC with atomic percentages of 57.6% and 42.4%, respectively (Figure 2D). These results are consistent with Lee *et al.*⁴⁹ and Tsunekawa *et al.*⁵⁰, reporting higher Ce³⁺ concentration at the surface of the CeO₂-NPs as size decreases below 10 nm. The coexistence of two oxidation states confers strong enzyme-mimicking antioxidant property on CeO₂-NPs. 51,52

3.2 Nanoceria localization in seed tissues

2

4 5 6

7

8

Tisology Of Misphigh

38

39 40

47 48

49 50 51

52 53

54 55

56 57 58

59 60

The distribution of nanoceria in seed tissues was evaluated by confocal fluorescence microscopy after incubating seeds in the presence of PNC labeled with a fluorescent dye Dil (Dil-PNC) in DI water (500 mg/L, 24 h). Although most Dil-PNC accumulated in the seed coat inner tegmen, nanoceria was also detected in the cotyledon and radicle (Figure 3). No Dil-PNC fluorescence signal was detected in control tissues exposed to distilled water (Figure S1). Orthogonal views in the confocal images indicate that the majority of the nanoceria distribute in the region of the root apical meristem (RAM) (Figure 3C). PNC's smaller size (2.1 ± 1.4 nm) than reported plant cell wall pore size⁵³ and high zeta potential (-51.7 ± 11.5 mV) facilitate the translocation across plant lipid bilavers^{54,55} and may allow PNC to distribute into the RAM. The RAM comprises undifferentiated cells that give rise to root tissues in seedlings under sustained cell division and differentiation.⁵⁶ Plant hormone signaling⁵⁷, transcriptional networks^{56,58}, ROS⁵⁹, and environmental cues⁶⁰ have been implicated in controlling the different zones of the RAM that regulate root development. Therefore, we assessed if seed priming impacted the root phenotype and physiological pathways in seedlings under salinity stress.

3.3 Influence of nanoceria seed priming on seedling phenotype

PNC priming had no effect on the percentage of seed germination under salinity stress (Figure 4A), but improved seedling development by increasing root length (56%), fresh (41%), and dry weight (38%) (Figure 4B-E) (P < 0.05). The cotyledon and hypocotyl biomass were not influenced by PNC priming under salinity stress (Figure S2). Cotton

*⊉*6

 seed germination and emergence of seedlings are generally delayed and reduced by salinity stress, even though the variety used herein (Acala 1517) is more tolerant at germination stage.^{30,31} Similarly, CeO₂ NPs (7 nm, 500-4000 mg/L) have been reported to have no effect on soybean germination, but instead enhanced plant root elongation.⁶¹ In *Arabidopsis* plants, leaves embedded with PNC (10 ± 0.6 nm, -17 ± 2.7 mV, 50 mg/L) exhibit improved shoot biomass under 100 mM NaCl for two weeks compared with plants without nanoparticles controls.²¹ Rice seedlings exposed to CeO₂ NPs (620.73 ± 50.31 nm, -11.63 ± 0.32 mV, 200 mg/L) experience alleviated salt stress (50 mM NaCl) as measured by shoot height and fresh weight.²⁸ Polyvinylpyrrolidone (PVP) coated CeO₂ NPs (55.6 nm, -51.8 mV, 200 and 1000 mg/L) increased both plant fresh weight and dry weight of canola (*Brassica napus* L.) under 100 mM NaCl.²⁶ These results indicate that nanoceria does not impact seed germination but influences the development and physiology of seedling after the exposure to nanoparticles at the seed stage.

Root phenotype showed the strongest impact by PNC seed priming under salinity stress. The PNC treated seeds developed into seedlings with longer and thinner roots than controls without nanoparticles (Figure 4F). The root system plays a critical role in response to abiotic stress⁶²; in some plants, response to salinity includes increasing their root growth at early stages of abiotic stress.^{30,31} Salinity stress significantly increased the total seedling root area relative to water control but not the vascular cylinder area and xylem area (P < 0.05) (Figure 4G, H, and I). In contrast, we observed a significant decrease in total root area (42%), vascular cylinder area (38%), and xylem

Tisology Also Associated the second of the s

*⊉*6

 element area (47%) in seedlings grown from PNC prime seeds relative to controls without nanoparticles (P < 0.05) (Figure 4 F, G, H, and I). A quantitative assessment of root vitality by changes in 2, 3, 5-triphenyltetrazolium chloride (TTC) intensity indicated that PNC priming improves seedling root vitality under salt stress conditions (114%, P < 0.05) (Figure S3A, B). The colorless TTC is reduced to the red-colored triphenyl formazan as a result of the dehydrogenase activity in the mitochondrial respiratory chain, serving as an indicator of root vitality. 39,40,63 Together these results indicate that PNC priming leads to increases in root length, biomass, and root vitality with associated modifications to root anatomical structure that increase seedling salinity tolerance.

3.4 Nanoceria seed priming reduces seedling ROS levels

PNC seed priming results in a significant decrease in ROS levels (63%, P < 0.05) in seedlings under salinity stress (Figure 5A, C). The decrease in ROS in roots induced by PNC seed priming was confirmed by staining with H₂DCFDA, an ROS indicator that converts to its fluorescent DCF form upon reaction with ROS⁴³ (Figure 5B, D). PNC (10 \pm 0.6 nm, -17 \pm 2.7 mV) have been demonstrated to be potent scavengers of H₂O₂ in stressed *Arabidopsis* plants *in vivo*.^{20,21} However, the Ce content in roots of cotton seedlings assessed by elemental analysis was below the detection limit, indicating that in this study it was likely not ROS scavenging by PNC in the seedling but seed priming with PNC that led to changes in the antioxidant enzymatic activity. Seed priming treatments with H₂O₂, 24-epibrassinolide, or zinc oxide nanoparticles have been reported to increase the activities of antioxidant enzymes (catalase, peroxidase, and superoxide dismutase)^{6,64} and antioxidant compounds (ascorbic acid and reduced

4 5

6

7

8

38 39

40 41

42 43

44 45 46

47 48

49 50

51 52

53 54 55

56 57 58

59 60 glutathione)^{6,11} involved in scavenging of ROS.^{5,32} Thus the effect of PNC seed priming on seedling performance is expected to be associated with improvement in the activity of antioxidant metabolic pathways.

3.6 Seedling tissue ion content in response to nanoceria seed priming

The content of key elements (Na, K, Ca and Mg) involved in plant signaling, enzyme activity, and ion homeostasis 65-70 were measured by inductively coupled plasma optical emission spectroscopy (ICP-OES) in seedling organs including cotyledons, hypocotyls, and roots (Figure 6). Previous studies have reported that CeO₂ NPs decrease root apoplastic barriers, which allows more Na⁺ transport to shoots and less accumulation of Na⁺ in plant roots, improving *Brassica napus* L. salt stress tolerance.²⁷ As expected, salinity stress increased Na content in seedlings. However, there were no significant differences in Na content for cotyledons, hypocotyls, and roots between PNC priming and controls (Figure 6A). Plant tissue K⁺ homeostasis is important to metabolic activity and salinity tolerance. 25,68,71,72 K+ is involved in osmotic adjustment and maintenance of cell turgor in salt-stressed plants. 65,66 In this study, no major differences in K content of cotyledons and hypocotyls was noted, except for a slightly lower K content in roots of PNC seed primed plants under salt stress (6%, P < 0.05) (Figure 6B). Thus, K homeostasis may not be the main mechanism involved in PNC priming enhancement of seedling salinity-tolerance. In contrast, PNC seed priming significantly increased (P < 0.05) the Ca content in cotyledons (28%), hypocotyls (58%), and roots (22%) under salt stress relative to water controls (Figure 6C). Ca2+ is a conserved secondary messenger that plays essential roles in the signal perception and transduction, and provides salinity

3.7 Differentially expressed genes (DEGs) in seedling roots

2

4 5

6

7

8

Tisology Also Associated the second of the s

38 39

40 41

42 43

44 45 46

47 48

49 50

51 52 53

54 55

56 57 58

59 60 To understand the molecular mechanisms mediating how PNC seed priming leads to phenotypic and physiological changes in seedling root development under salt stress, we used high-throughput RNA sequencing (RNA-seq) to assess gene expression profiles in roots over time. We performed transcriptomic analysis to assess the impact of interfacing PNC seeds on the expression of genes associated with antioxidant activity and ion homeostasis. A total 42 sequencing libraries (14 treatment with 3 biological replications) were constructed from seedling root samples. Pearson's correlation coefficient between biological replications was high (0.975) (Figure S4).^{77,78} A total of 4,779 genes showed differential expression between PNC priming alone and no nanoparticle water control treatments under normal conditions (Figure S5A). About 275

4 5

6

7

8

14:46.PM6 1 0

1:80202/52/9 or or osipwall 1:80203/3/2/9 or osipwall 2:803/3/2/9 or osipwall 2:803/3/2/9 or osipwall 3:803/3/2/9 or osipwall 3:803/3/9 or osipwall 3:

*⊉*6

38 39

40 41

42 43

44 45 46

47 48

49 50

51 52 53

54 55

56 57 58

59 60 DEGs were identified when comparing PNC priming treatments for salinity stress and water controls, of which 68, 10, 134 and 51 DEGs were detected at 0, 12, 24 and 48 h, respectively (Figure S5B). From these DEGs, 13 were related to ROS pathways (Figure 7A) and 10 to ion homeostasis (Figure 7B).

3.8 PNC seed priming regulates genes related to scavenging of ROS under salinity stress

Salinity stress induces the accumulation of ROS, which leads to oxidative stress. disruption of cellular redox homeostasis, and damage to cell structure. 79-81 To alleviate oxidative damage, plants have enzymatic antioxidant systems that include peroxidases (POD), glutathione S-transferases (GST), and peroxiredoxins (PRX). 30,70,80,81 A total of 7 peroxidase POD genes (Gh. A03G2152, Gh. A03G1517, Gh. D08G2330, Gh A09G1415, Gh D09G1420, Gh A10G2288, and Gh D11G2183) were significantly up-regulated by PNC priming when comparing seedlings under salt stress (24 h) with water controls (Figure 7A). POD are mainly located in the apoplastic space and cell vacuole, where they play an important role in catalyzing H₂O₂ to H₂O and O₂.81 A total of 23 members of the POD family are up-regulated upon salinity stress in wild cotton (Gossypium klotzschianum), a cultivar with improved salt tolerance.⁷⁹ PNC priming under salinity stress also upregulates 2 glutathione S-transferase GST tau (GSTU7 Gh A02G0259 and GSTU8 Gh A09G1508) and downregulates a pair of GSTU17 (Gh A11G3130, and Gh D11G3426) (48 h) (Figure 7A). Increased GST expression levels protect organisms against oxidative stress. AtGSTU7 is strongly expressed in response to multiple stresses,82 and GSTU8 has high peroxidase activity.83 However,

14:46.PM6 1 0

1:8 0202/2020 or or osipeW 2 3 4 5 6 7 8

*⊉*6

 AtGSTU17 plays a negative role in salt stress tolerance.⁸⁴ A pair of peroxiredoxin *PRX* (*Gh_A10G1567*, and *Gh_D10G1825*) genes were significantly down-regulated by PNC priming comparing salinity stress treatment (48 h) with water controls (Figure 7A). PRXs are a group of thiol-specific antioxidant enzymes that are differentially regulated under stress-inducing conditions.⁸⁵ Overall, the transcriptomic analysis indicates that PNC seed priming enhances salinity tolerance of seedlings through changes in the expression of ROS enzymatic gene families, including *POD*, *GST*, and *PRX*.

3.9 PNC seed priming regulates genes related to ion binding and transport under salinity stress

Salinity stress induces accumulation of Na⁺ and loss of K⁺. Our transcriptomic analysis indicates that the K⁺ channel *AKT1* (*Gh_A13G1762*) gene was significantly down-regulated by PNC seed priming under salinity stress compared with water controls (48 h) (Figure 7B). This is consistent with root K content in PNC priming treatments being slightly lower in salinity stress conditions than in water controls (Figure 6B).

Ca²⁺ is a key messenger in signaling salt stress. We found that the cation exchanger (CAX1) gene *GhCAX1* (*Gh_D01G0422*) was down-regulated by PNC priming when comparing salinity stress treated seedlings with water controls (48 h) (Figure 7A). CAX1 transporter is an important transporter located in the vacuole that regulates the amplitude and duration of cytosolic Ca²⁺ levels. A high expression level of CAX1 causes salt sensitivity.⁸⁶ Thus, our results indicate that PNC seed priming enhances salt

*⊉*6

 tolerance in cotton seedlings through the down-regulation of *CAX1* that increases cytosolic Ca²⁺ levels. Furthermore, a pair of calcium-binding EF-hand family protein gene *EF-hand* (*Gh_A07G1532*, and *Gh_D07G1690*) were up-regulated (0 h) and *EF-hand* (*Gh_D07G2171*) were down-regulated (24 h) by PNC priming when comparing salinity stressed seedlings with water controls (Figure 7B). The EF-hand motif is a helix-loop-helix structure that binds a single Ca²⁺ ion.⁸⁷ Differential expression of EF-hand family transgenes has been reported to increase drought and salinity tolerance of *Arabidopsis* genetically modified plants⁸⁸ and soybean crops.⁸⁹ Transient and minor changes of Ca²⁺ caused by extracellular stimuli, such as PNC in the root apical meristem, could be detected and transduced by Ca²⁺ sensors or Ca²⁺-binding proteins, and lead to strong responses of downstream factors.⁶⁷

A total of 5 DEGs associated with Mg²⁺ ion binding for terpene synthase (TPS) were detected when comparing salinity stress PNC priming treatments and water controls (Figure 7B). From these 5 DEGs, 3 (+)-δ-cadinene synthase isozyme A genes *CAD1s* (*Gh_A01G1712*, *Gh_D01G1963*, and *Gh_D13G1503*) and one terpene synthase *TPS9* gene (*Gh_D05G2768*) were up-regulated by PNC priming. The three *CAD1s* were up-regulated before and after 24 h after salinity stress. Only one sesquiterpene synthase gene *TPS1* (*Gh_A01G0555*) was down-regulated by PNC priming under salinity stress (48 h). Terpenoids constitute a large class of compounds that play roles in plant defense against biotic and abiotic stresses.⁹⁰ Plant hormones associated with stress responses including ABA, GAs, CKs, and strigolactones are made in whole or in part by terpenes.⁹¹ In cotton, gossypol and related sesquiterpene phytoalexins that protect

4 Conclusion

2

4 5

6

7

8

38 39

40 41

42 43 44

45 46

47 48

49 50 51

52 53

54 55

56 57 58

59 60 PNC seed priming improves cotton root development under salinity stress by modulating underlying molecular mechanisms affecting root morphological. physiological, and biochemical responses (Figure 8). Maintenance of root vitality. changes in root anatomical structure, and increases in root biomass by PNC seed priming are associated with seedling reduction of ROS and increase in calcium and magnesium levels. PNC localized in cotton seed tissues but not in seedlings, indicating that PNC seed priming but not ROS scavenging in seedlings affects gene expression of ROS enzymatic pathways (POD, GST, and PRX families), calcium transporter CAX1 and calcium-binding EF-hand family genes. Both ROS and Ca²⁺ are part of conserved signaling pathways involved in detection and transduction of stress responses in plants.67,81,95 Thus ROS and Ca²⁺ mediated signaling could be part of a unifying mechanism of nanoparticle seed priming effects on seedling performance under stress. PNC priming also increases Mg content in roots of cotton seedlings, and up-regulates terpene synthase genes (CAD1 and TPS) that enhances salinity stress tolerance in cotton. This study elucidates molecular mechanisms mediating how PNC seed priming

Tisto of Missonian

*⊉*6

 modifies cotton seedling development under salinity stress through signaling ion and antioxidant pathways. Investigating the impact of seed priming with antioxidant nanoparticles in controlled facilities on seedling stress performance in field conditions will elucidate nano-enabled technologies that minimize nanoparticle exposure to onfarm workers, consumers, and the environment. Nanoparticle seed priming provides a sustainable, practical and scalable tool for improving crop tolerance to stress during the critical seedling development stage.

Conflicts of interest

The authors declare no competing financial interests.

Acknowledgments

This work was supported by the National Science Foundation under the Center for Sustainable Nanotechnology, CHE-1503408. The CSN is part of the Centers for Chemical Innovation Program. RNA-seq analysis was funded through support from the National Key Research and Development Program of China (Grant No. 2018YFD1000903). JA was supported by the Chinese Scholarship Council Fellowship program. Cotton seeds (Acala 1517-08) were provided by Prof. Jinfa Zhang in Department of Plant and Environmental Sciences, New Mexico State University. XPS measurements were performed using the Kratos AXIS ULRTADLD XPS system which is supported by NSF DMR-0958796.

Figure legends

 Figure 1. Cerium oxide nanoparticles (PNC) influence on cotton seedling development under salinity stress. Interfacing PNC with seeds grown under salinity stress (200 mM NaCl) affects reactive oxygen species (ROS) dependent pathways related genes (peroxidase *POD* genes), and Ca²⁺, and Mg²⁺ ion homeostasis. These molecular changes in seedling development improve root development and tolerance to salt stress.

Figure 2. Characterization of cerium oxide nanoparticles (PNC). A, Hydrodynamic diameter measured by DLS in DI water (pH 8), **B**, representative TEM image, **C**, zeta potential, and **D**, XPS spectra showing $Ce(III) = u' + u_0 + v' + v_0$ and Ce(IV) = u''' + u'' + u''' + v''' + v. Error bar represents standard deviation, n = 3.

Figure 3. Cerium oxide nanoparticle (PNC) localization in cotton seed tissues. Confocal fluorescence microscopy images after 24 h priming with PNC labeled with the fluorescent dye Dil (green). The nanoparticles were localized in the $\bf A$, seed coat within the inner tegmen, $\bf B$, in cotyledons, and $\bf C$, the radicle. Scale bar = 50 μ m. $\bf D$, Schematic diagram of cotton seed structure.

Figure 4. Modification of seedling root development under salinity stress by cerium oxide nanoparticles (PNC). A, PNC do not impact seed germination rates

14:46.PM6 1 0

Tisology Also Associated the second of the s

*⊉*6

 under salinity stress (200 mM NaCl). **B**, PNC modify root development by enhancing root **C**, length, **D**, fresh weight, and **E**, dry weight, as shown with box plots. **F**, Representative cross sections of cotton roots stained with toluidine blue. The changes in root morphology and biomass are accompanied by reductions in **G**, root cross sectional area, **H**, vascular cylinder and **I**, xylem area. Boxes represent the interquartile range from the first to the third quartile with squares as the medians. Statistical comparisons were performed by independent samples one-way ANOVA on Duncan's test (two tailed) or Kruskal Wallis test. Data with different lowercase letters indicate significant differences (P < 0.05). Error bars indicate standard deviation, $n \ge 4$.

Figure 5. ROS scavenging by cerium oxide nanoparticles (PNC) in cotton seedling roots under salinity stress. A, Representative DAB staining images reflecting hydrogen peroxide levels in cotton seedling root tips. B, Confocal microscopy images of DCF fluorescent dye indicating ROS levels in cotton seedling root maturation zone. Quantitative analysis of \mathbf{C} , DAB staining intensities in cotton root tip and \mathbf{D} , area normalized DCF intensity in cotton root maturation zone. Boxes represent the interquartile range from the first to the third quartile with squares as the medians. Statistical comparisons were performed by independent samples one-way ANOVA on Duncan's test (two tailed). Data with different lowercase letters indicate significant differences (P < 0.05). Error bars indicate standard deviation, n = 5.

Figure 6. Effect of cerium oxide nanoparticles (PNC) on ion content in cotton seedlings exposed to salt stress. Concentration of A, Na, B, K, C, Ca, and D, Mg in

cotton seedling cotyledons, hypocotyls and roots, lon content levels were measured by ICP-OES. Statistical comparisons were performed by independent samples one-way ANOVA on Duncan's test (two tailed) or Kruskal Wallis test. Data with different lowercase letters indicate significant differences (P < 0.05). Error bars indicate standard error, $n \ge 3$.

2 3

4 5

6

7

8

14:46.PM6 1 0

1:8 0202/2020 or or osipeW 2 3 4 5 6 7 8

Tisology Also Associated the second of the s

*⊉*6

38

39 40 41

42 43

44 45

46 47

54 55

56 57 58

59 60 Figure 7. Expression profiling of genes related to ion homeostasis and ROS pathway. Heat maps showing the expression level (log₁₀(FPKM + 0.001), FPKM, fragments per kilobase of exon model per million mapped reads) of differentially expressed genes (DEG). Numbers are indicated at time points when the transcript expression level between PNC priming and water control was significantly different (n = 3. adjusted P-value < 0.05 and fold change \geq 1). RNA-seg analysis of genes associated with **A**, ROS related enzymes POD, GST, and PRX, **B**, K⁺, Ca²⁺, and Mg²⁺ homeostasis. W0: after H₂O priming and before salinity stress. P0: after PNC priming and before salinity stress. W12, W24, W48: after H₂O priming and grown under normal conditions for 12, 24 and 48 h, respectively. P12, P24, P48: after PNC priming and grown under normal conditions for 12, 24 and 48 h, respectively. WS12, WS24, WS48: after H₂O priming and grown under salinity stress for 12, 24 and 48 h, respectively. PS12, PS24, PS48: after PNC priming and grown under salinity stress for 12, 24 and 48 h, respectively.

Figure 8. Molecular interaction network of how cerium oxide nanoparticles (PNC) impact cotton seedling development under salinity stress. Salinity stress induce ion

 stress and oxidative burst, increase the H_2O_2 in plant cell. PNC priming influences ion homeostasis (Ca^{2+} , and Mg^{2+}), boosts the ROS pathway, and stress defense response that results in improved cotton seedling salinity tolerance. Up-regulated genes (green with upward-pointing arrows) and down-regulated genes (red with downward-pointing arrows) at a given time point.

References

- S. Hussain, M. Zheng, F. Khan, A. Khaliq, S. Fahad, S. Peng, J. Huang, K. Cui and L. Nie, Benefits of rice seed priming are offset permanently by prolonged storage and the storage conditions, *Sci. Rep.*, 2015, **5**, 8101.
- 2 S. Hussain, F. Khan, H. A. Hussain and L. Nie, Physiological and biochemical mechanisms of seed priming-induced chilling tolerance in rice cultivars, *Front. Plant Sci.*, 2016, **7**, 116.
- S. Hussain, F. Khan, W. Cao, L. Wu and M. Geng, Seed priming alters the production and detoxification of reactive oxygen intermediates in rice seedlings grown under sub-optimal temperature and nutrient supply, *Front. Plant Sci.*, 2016, 7, 439.
- 4 A. Savvides, S. Ali, M. Tester and V. Fotopoulos, Chemical priming of plants against multiple abiotic stresses: mission possible?, *Trends Plant Sci.*, 2016, **21**, 329–340.

6 7

8

14:46.PM6 1 0

Tisto of Missonian

*⊉*6

38 39 40

41 42 43

44 45

46 47

48 49 50

51 52

- S. Paparella, S. S. Araújo, G. Rossi, M. Wijayasinghe, D. Carbonera and A. Balestrazzi, Seed priming: state of the art and new perspectives, *Plant Cell Rep.*, 2015, 34, 1281–1293.
- H. Ellouzi, S. Sghayar and C. Abdelly, H₂O₂ seed priming improves tolerance to salinity; drought and their combined effect more than mannitol in *Cakile maritima* when compared to *Eutrema salsugineum*, *J. Plant Physiol.*, 2017, **210**, 38–50.
- S. Hussain, A. Khaliq, M. Tanveer, A. Matloob and H. A. Hussain, Aspirin priming circumvents the salinity-induced effects on wheat emergence and seedling growth by regulating starch metabolism and antioxidant enzyme activities, *Acta Physiol. Plant.*, 2018, **40**, 68.
- P. Wang, E. Lombi, F. J. Zhao and P. M. Kopittke, Nanotechnology: A new opportunity in plant sciences, *Trends Plant Sci.*, 2016, **21**, 699–712.
- 9 J. P. Giraldo, H. Wu, G. M. Newkirk and S. Kruss, Nanobiotechnology approaches for engineering smart plant sensors, *Nat. Nanotechnol.*, 2019, **14**, 541–553.
- M. Kah, N. Tufenkji and J. C. White, Nano-enabled strategies to enhance crop nutrition and protection, *Nat. Nanotechnol.*, 2019, **14**, 532–540.
- A. A. H. Abdel Latef, M. F. Abu Alhmad and K. E. Abdelfattah, The possible roles of priming with ZnO nanoparticles in mitigation of salinity stress in lupine (*Lupinus termis*) plants, *J. Plant Growth Regul.*, 2017, **36**, 60–70.
- F. R. Cassee, E. C. Van Balen, C. Singh, D. Green, H. Muijser, J. Weinstein andK. Dreher, Exposure, health and ecological effects review of engineered

5

6

7 8

14:46.PM6 1 0

1:80202/52/9 or or osipwall 1:80203/3/2/9 or osipwall 2:803/3/2/9 or osipwall 2:803/3/2/9 or osipwall 3:803/3/2/9 or osipwall 3:803/3/9 or osipwall 3:

Trismosymyo Alsahiny

⊉6

164 0024 June 2020 Dewnloaded

38 39 40

41 42

43 44 45

46 47

48 49

50 51 52

53 54 55

56 57 58

- nanoscale cerium and cerium oxide associated with its use as a fuel additive, *Crit.*Rev. Toxicol., 2011, 41, 213–229.
- Q. Wang, S. D. Ebbs, Y. Chen and X. Ma, Trans-generational impact of cerium oxide nanoparticles on tomato plants, *Metallomics*, 2013, 5, 753–759.
- 14 C. P. Andersen, G. King, M. Plocher, M. Storm, L. R. Pokhrel, M. G. Johnson and P. T. Rygiewicz, Germination and early plant development of ten plant species exposed to titanium dioxide and cerium oxide nanoparticles, *Environ. Toxicol. Chem.*, 2016, **35**, 2223–2229.
- 15 Q. Wang, X. Ma, W. Zhang, H. Pei and Y. Chen, The impact of cerium oxide nanoparticles on tomato (*Solanum lycopersicum* L.) and its implications for food safety, *Metallomics*, 2012, **4**, 1105–1112.
- 16 C. M. Rico, M. I. Morales, A. C. Barrios, R. McCreary, J. Hong, W. Y. Lee, J. Nunez, J. R. Peralta-Videa and J. L. Gardea-Torresdey, Effect of cerium oxide nanoparticles on the quality of rice (*Oryza sativa* L.) grains, *J. Agric. Food Chem.*, 2013, 61, 11278–11285.
- A. Dhall and W. Self, Cerium oxide nanoparticles: A brief review of their synthesis methods and biomedical applications, *Antioxidants*, 2018, **7**, 97.
- 18 B. C. Nelson, M. E. Johnson, M. L. Walker, K. R. Riley and C. M. Sims,
 Antioxidant cerium oxide nanoparticles in biology and medicine, *Antioxidants*,
 2016, **5**, 15.
- J. P. Giraldo, M. P. Landry, S. M. Faltermeier, T. P. McNicholas, N. M. Iverson, A.A. Boghossian, N. F. Reuel, A. J. Hilmer, F. Sen, J. A. Brew and M. S. Strano,

6

7 8

14:46.PM6 1 0

⊉6

38 39 40

41 42 43

44 45

46 47 48

49 50

51 52

- Plant nanobionics approach to augment photosynthesis and biochemical sensing, *Nat. Mater.*, 2014, **13**, 400–408.
- 20 H. Wu, N. Tito and J. P. Giraldo, Anionic cerium oxide nanoparticles protect plant photosynthesis from abiotic stress by scavenging reactive oxygen species, *ACS Nano*, 2017, **11**, 11283–11297.
- 21 H. Wu, L. Shabala, S. Shabala and J. P. Giraldo, Hydroxyl radical scavenging by cerium oxide nanoparticles improves *Arabidopsis* salinity tolerance by enhancing leaf mesophyll potassium retention, *Environ. Sci. Nano*, 2018, **5**, 1567–1583.
- L. Tumburu, C. P. Andersen, P. T. Rygiewicz and J. R. Reichman, Phenotypic and genomic responses to titanium dioxide and cerium oxide in *Arabidopsis* germinants, *Environ. Toxicol. Chem.*, 2015, **34**, 70–83.
- H. Zhang, L. Lu, X. Zhao, S. Zhao, X. Gu, W. Du, H. Wei, R. Ji and L. Zhao, Metabolomics reveals the 'invisible' responses of spinach plants exposed to CeO₂ nanoparticles, *Environ. Sci. Technol.*, 2019, **53**, 6007–6017.
- J. K. Zhu, Plant salt tolerance, *Trends Plant Sci.*, 2001, **6**, 66–71.
- L. Zhang, H. J. Ma, T. T. Chen, J. Pen, S. X. Yu and X. H. Zhao, Morphological and physiological responses of cotton (*Gossypium hirsutum* L .) plants to salinity, *PLoS One*, 2014, **9**, e112807.
- 26 L. Rossi, W. Zhang, L. Lombardini and X. Ma, The impact of cerium oxide nanoparticles on the salt stress responses of *Brassica napus* L., *Environ. Pollut.*, 2016, 219, 28–36.

6

7

8

14:46.PM6 1 0

Trismosymyo Aksaniny

*⊉*6

below of the contraction of the

38 39 40

41 42 43

44 45

46 47 48

49 50

- 27 L. Rossi, W. Zhang and X. Ma, Cerium oxide nanoparticles alter the salt stress tolerance of *Brassica napus* L. by modifying the formation of root apoplastic barriers, *Environ. Pollut.*, 2017, 229, 132–138.
- Y. Y. Wang, L. Q. Wang, C. X. Ma, K. X. Wang, Y. Hao, Q. Chen, Y. Mo and Y. K. Rui, Effects of cerium oxide on rice seedlings as affected by co-exposure of cadmium and salt, *Environ. Pollut.*, 2019, **252**, 1087–1096.
- 29 S. Ahmad, N.-I. Khan, M. Z. Iqbal, A. Hussain and M. Hassan, Salt tolerance of cotton (*Gossypium hirsutum* L.), *Asian J. Plant Sci.*, 2002, **1**, 715–719.
- A. Abdelraheem, N. Esmaeili, M. O'Connell and J. Zhang, Progress and perspective on drought and salt stress tolerance in cotton, *Ind. Crops Prod.*, 2019, 130, 118–129.
- 31 M. Ashraf, Salt tolerance of cotton: Some new advances, *CRC. Crit. Rev. Plant Sci.*, 2002, **21**, 1–30.
- 32 E. A. Ibrahim, Seed priming to alleviate salinity stress in germinating seeds, *J. Plant Physiol.*, 2016, **192**, 38–46.
- 33 K. D. Schierbaum, Ordered ultra-thin cerium oxide overlayers on Pt (III) single crystal surfaces studied by LEED and XPS, Surf. Sci., 1998, 399, 29–38.
- E. Bêche, P. Charvin, D. Perarnau, S. Abanades and G. Flamant, Ce 3d XPS investigation of cerium oxides and mixed cerium oxide (Ce_xTi_yO_z), *Surf. Interface Anal.*, 2008, **40**, 264–267.

- 35 C. Anandan and P. Bera, XPS studies on the interaction of CeO₂ with silicon in magnetron sputtered CeO₂ thin films on Si and Si₃N₄ substrates, *Appl. Surf. Sci.*, 2013, **283**, 297–303.
- 36 E. J. Preisler, O. J. Marsh, R. A. Beach and T. C. McGill, Stability of cerium oxide on silicon studied by x-ray photoelectron spectroscopy, *J. Vac. Sci. Technol. B*, 2001, **19**, 1611–1618.
- A. Asati, S. Santra, C. Kaittanis and J. M. Perez, Surface-charge-dependent cell localization and cytotoxicity of cerium oxide nanoparticles, *ACS Nano*, 2010, **4**, 5321–5331.
- P. Pradhan Mitra and D. Loqué, Histochemical staining of *Arabidopsis thaliana* secondary cell wall elements, *J. Vis. Exp.*, 2014, e51381.
- 39 L. H. Comas, D. M. Eissenstat and A. N. Lakso, Assessing root death and root system dynamics in a study of grape canopy pruning, *New Phytol.*, 2000, **147**, 171–178.
- J. Jiang, M. Su, L. Wang, C. Jiao, Z. Sun, W. Cheng, F. Li and C. Wang, Exogenous hydrogen peroxide reversibly inhibits root gravitropism and induces horizontal curvature of primary root during grass pea germination, *Plant Physiol. Biochem.*, 2012, **53**, 84–93.
- D. Kumar, M. A. Yusuf, P. Ringh, M. Sardar and N. B. Sarin, Histochemical detection of superoxide and H₂O₂ accumulation in *Brassica juncea* seedlings, *Bioprotocol*, 2014, **17**, e1108.

Tisology Also Associated the second of the s

*⊉*6

- 43 K. A. Kristiansen, P. E. Jensen, I. M. Møller and A. Schulz, Monitoring reactive oxygen species formation and localisation in living cells by use of the fluorescent probe CM-H2DCFDA and confocal laser microscopy, *Physiol. Plant.*, 2009, **136**, 369–383.
- C. Ma, J. Borgatta, R. De La Torre-Roche, N. Zuverza-Mena, J. C. White, R. J. Hamers and W. H. Elmer, Time-dependent transcriptional response of tomato (Solanum lycopersicum L.) to Cu nanoparticle exposure upon infection with Fusarium oxysporum f. sp. lycopersici, ACS Sustain. Chem. Eng., 2019, 7, 10064–10074.
- J. Borgatta, C. Ma, N. Hudson-Smith, W. Elmer, C. D. Plaza Pérez, R. De La Torre-Roche, N. Zuverza-Mena, C. L. Haynes, J. C. White and R. J. Hamers, Copper based nanomaterials suppress root fungal disease in watermelon (*Citrullus lanatus*): Role of particle morphology, composition and dissolution behavior, *ACS Sustain. Chem. Eng.*, 2018, 6, 14847–14856.
- W. H. Elmer and J. C. White, The use of metallic oxide nanoparticles to enhance growth of tomatoes and eggplants in disease infested soil or soilless medium, *Environ. Sci. Nano*, 2016, **3**, 1072–1079.

*⊉*6

- T. Zhang, Y. Hu, W. Jiang, L. Fang, X. Guan, J. Chen, J. Zhang, C. A. Saski, B. E. Scheffler, D. M. Stelly, A. M. Hulse-Kemp, Q. Wan, B. Liu, C. Liu, S. Wang, M. Pan, Y. Wang, D. Wang, W. Ye, L. Chang, W. Zhang, Q. Song, R. C. Kirkbride, X. Chen, E. Dennis, D. J. Llewellyn, D. G. Peterson, P. Thaxton, D. C. Jones, Q. Wang, X. Xu, H. Zhang, H. Wu, L. Zhou, G. Mei, S. Chen, Y. Tian, D. Xiang, X. Li, J. Ding, Q. Zuo, L. Tao, Y. Liu, J. Li, Y. Lin, Y. Hui, Z. Cao, C. Cai, X. Zhu, Z. Jiang, B. Zhou, W. Guo, R. Li and Z. J. Chen, Sequencing of allotetraploid cotton (*Gossypium hirsutum L.* acc. TM-1) provides a resource for fiber improvement, *Nat. Biotechnol.*, 2015, 33, 531–537.
- 48 N. Carpita, D. Sabularse, D. Montezinos and D. P. Delmer, Determination of the pore size of cell walls of living plant cells, *Science*, 1979, **205**, 1144–1147.
- 49 S. S. Lee, W. Song, M. Cho, H. L. Puppala, P. Nguyen, H. Zhu, L. Segatori and V. L. Colvin, Antioxidant properties of cerium oxide nanocrystals as a function of nanocrystal diameter and surface coating, *ACS Nano*, 2013, 7, 9693–9703.
- 50 S. Tsunekawa, R. Sivamohan, S. Ito, A. Kasuya and T. Fukuda, Structural study on monosize CeO_{2-X} nano-particles, *Nanostructured Mater.*, 1999, **11**, 141–147.
- Y. Yang, Z. Mao, W. Huang, L. Liu, J. Li, J. Li and Q. Wu, Redox enzymemimicking activities of CeO₂ nanostructures: Intrinsic influence of exposed facets, *Sci. Rep.*, 2016, **6**, 35344.
- A. Trovarelli and J. Llorca, Ceria catalysts at nanoscale: How do crystal shapes shape catalysis?, *ACS Catal.*, 2017, **7**, 4716–4735.

5

6 7

8

14:46.PM6 1 0

Tisto of Missonian

*⊉*6

Published on 24 June 2020 Dewnloaded 2020 Dewnloaded 2020 Develoaded 2020 Dewnloaded 2020 Dewn

38 39 40

41 42 43

44 45

46 47 48

49 50

51 52 53

- P. Albersheim, A. Darvill, K. Roberts, R. Sederoff and A. Staehelin, *Plant cell walls: from chemistry to biology. Garland Science*, New York (USA), 2010.
- M. H. Wong, R. P. Misra, J. P. Giraldo, S. Y. Kwak, Y. Son, M. P. Landry, J. W. Swan, D. Blankschtein and M. S. Strano, Lipid exchange envelope penetration (LEEP) of nanoparticles for plant engineering: A universal localization mechanism, *Nano Lett.*, 2016, **16**, 1161–1172.
- T. T. S. Lew, M. H. Wong, S. Y. Kwak, R. Sinclair, V. B. Koman and M. S. Strano, Rational design principles for the transport and subcellular distribution of nanomaterials into plant protoplasts, *Small*, 2018, **14**, 1802086.
- S. Perilli, R. Di Mambro and S. Sabatini, Growth and development of the root apical meristem, *Curr. Opin. Plant Biol.*, 2012, **15**, 17–23.
- 57 Z. Y. Wei and J. Li, Brassinosteroids regulate root growth, development, and symbiosis, *Mol. Plant*, 2016, **9**, 86–100.
- 58 R. C. Drisch and Y. Stahl, Function and regulation of transcription factors involved in root apical meristem and stem cell maintenance, *Front. Plant Sci.*, 2015, **6**, 505.
- 59 H. Tsukagoshi, Control of root growth and development by reactive oxygen species, *Curr. Opin. Plant Biol.*, 2016, **29**, 57–63.
- 60 H. Motte, S. Vanneste and T. Beeckman, Molecular and environmental regulation of root development, *Annu. Rev. Plant Biol.*, 2019, **70**, 465–488.
- M. L. López-Moreno, G. De La Rosa, J. A. Hernández-Viezcas, H. Castillo-Michel,C. E. Botez, J. R. Peralta-Videa and J. L. Gardea-Torresdey, Evidence of the

6

7 8

14:46.PM6 1 0

1:8 0202/2020 or or osipeW 2 3 4 5 6 7 8

Tisology Also Associated to the second of th

*⊉*6

38 39 40

41 42

43

44 45

46 47

48 49 50

51 52

53 54 55

56 57 58

- differential biotransformation and genotoxicity of ZnO and CeO₂ nanoparticles on soybean (*Glycine max*) plants, *Environ. Sci. Technol.*, 2010, **44**, 7315–7320.
- G. Céccoli, J. C. Ramos, L. I. Ortega, J. M. Acosta and M. G. Perreta, Salinity induced anatomical and morphological changes in *Chloris gayana* Kunth roots, *Biocell*, 2011, **35**, 9–17.
- A. Higa, Y. Mori and Y. Kitamura, Iron deficiency induces changes in riboflavin secretion and the mitochondrial electron transport chain in hairy roots of Hyoscyamus albus, *J. Plant Physiol.*, 2010, **167**, 870–878.
- 64 F. Ozdemir, M. Bor, T. Demiral and I. Turkan, Effects of 24-epibrassinolide on seed germination, seedling growth, lipid peroxidation, proline content and antioxidative system of rice (*Oryza sativa* L.) under salinity stress, *Plant Growth Regul.*, 2004, 42, 203–211.
- 65 M. Wang, Q. Zheng, Q. Shen and S. Guo, The critical role of potassium in plant stress response, *Int. J. Mol. Sci.*, 2013, **14**, 7370–7390.
- I. Cakmak, The role of potassium in alleviating detrimental effects of abiotic stresses in plants, *J. Plant Nutr. Soil Sci.*, 2005, 168, 521–530.
- W. Gao, F. Xu, D. Guo, J. Zhao, J. Liu, Y. Guo, P. K. Singh, X. Ma, L. Long, J. R. Botella and C. Song, Calcium-dependent protein kinases in cotton: insights into early plant responses to salt stress, *BMC Plant Biol.*, 2018, 18, 15.
- A. K. Parida, A. B. Das and B. Mittra, Effects of salt on growth, ion accumulation, photosynthesis and leaf anatomy of the mangrove, *Bruguiera parviflora*, *Trees*, 2004, **18**, 167–174.

14:46.PM6 1 0

1:80202/52/9 or or osipwall 1:80203/3/2/9 or osipwall 2:803/3/2/9 or osipwall 2:803/3/2/9 or osipwall 3:803/3/2/9 or osipwall 3:803/3/9 or osipwall 3:

*⊉*6

- T. Kurusu, K. Kuchitsu and Y. Tada, Plant signaling networks involving Ca²⁺ and Rboh/Nox-mediated ROS production under salinity stress, *Front. Plant Sci.*, 2015, **6**, 427.
- M. A. Abid, C. Liang, W. Malik, Z. Meng, Z. Tao, Z. Meng, J. Ashraf, S. Guo and R. Zhang, Cascades of ionic and molecular networks involved in expression of genes underpin salinity tolerance in cotton, *J. Plant Growth Regul.*, 2018, **37**, 668–679.
- A. Wahid, M. Perveen, S. Gelani and S. M. A. Basra, Pretreatment of seed with H₂O₂ improves salt tolerance of wheat seedlings by alleviation of oxidative damage and expression of stress proteins, *J. Plant Physiol.*, 2007, **164**, 283–294.
- I. Tozlu, G. A. Moore and C. L. Guy, Effects of increasing NaCl concentration on stem elongation, dry mass production, and macro- and micro-nutrient accumulation in *Poncirus trifoliata*, *Aust. J. Plant Physiol.*, 2000, **27**, 35–42.
- N. Tuteja, Mechanisms of high salinity tolerance in plants, *Methods Enzymol.*, 2007, **428**, 419–438.
- M. M. Julkowska and C. Testerink, Tuning plant signaling and growth to survive salt, *Trends Plant Sci.*, 2015, **20**, 586–594.
- 75 I. C. Dodd and F. Pérez-Alfocea, Microbial amelioration of crop salinity stress, *J. Exp. Bot.*, 2012, **63**, 3415–3428.
- W. L. Guo, H. Nazim, Z. S. Liang and D. F. Yang, Magnesium deficiency in plants:

 An urgent problem, *Crop J.*, 2016, **4**, 83–91.

Tisology Also Associated to the second of th

- R. S. Sekhon, R. Briskine, C. N. Hirsch, C. L. Myers, N. M. Springer, C. R. Buell, N. de Leon and S. M. Kaeppler, Maize gene atlas developed by RNA sequencing and comparative evaluation of transcriptomes based on RNA sequencing and microarrays, *PLoS One*, 2013, 8, e61005.
- J. Huang, H. L. Wei, L. B. Li and S. X. Yu, Transcriptome analysis of nitric oxide-responsive genes in upland cotton (*Gossypium hirsutum*), *PLoS One*, 2018, **13**, e0192367.
- Y. Y. Wei, Y. C. Xu, P. Lu, X. X. Wang, Z. Q. Li, X. Y. Cai, Z. L. Zhou, Y. H. Wang, Z. M. Zhang, Z. X. Lin, F. Liu and K. B. Wang, Salt stress responsiveness of a wild cotton species (*Gossypium klotzschianum*) based on transcriptomic analysis, *PLoS One*, 2017, **12**, e0178313.
- I. Sharif, S. Aleem, J. Farooq, M. Rizwan, A. Younas, G. Sarwar and S. M. Chohan, Salinity stress in cotton: effects, mechanism of tolerance and its management strategies, *Physiol. Mol. Biol. Plants*, 2019, **25**, 807–820.
- L. X. Hu, H. Y. Li, H. C. Pang and J. M. Fu, Responses of antioxidant gene, protein and enzymes to salinity stress in two genotypes of perennial ryegrass (*Lolium perenne*) differing in salt tolerance, *J. Plant Physiol.*, 2012, **169**, 146–156.
- P. G. Sappl, A. J. Carroll, R. Clifton, R. Lister, J. Whelan, A. Harvey Millar and K. B. Singh, The *Arabidopsis* glutathione transferase gene family displays complex stress regulation and co-silencing multiple genes results in altered metabolic sensitivity to oxidative stress, *Plant J.*, 2009, **58**, 53–68.

14:46.PM6 1 0

Tisology Also Associated to the second of th

*⊉*6

- A. De Simone, R. Hubbard, N. V. De La Torre, Y. Velappan, M. Wilson, M. J. Considine, W. J. J. Soppe and C. H. Foyer, Redox changes during the cell cycle in the embryonic root meristem of *Arabidopsis thaliana*, *Antioxidants Redox Signal.*, 2017, 27, 1505–1519.
- J. H. Chen, H. W. Jiang, E. J. Hsieh, H. Y. Chen, C. Te Chien, H. L. Hsieh and T. P. Lin, Drought and salt stress tolerance of an arabidopsis glutathione S-transferase U17 knockout mutant are attributed to the combined effect of glutathione and abscisic acid, *Plant Physiol.*, 2012, **158**, 340–351.
- 85 F. J. Corpas, J. R. Pedrajas, J. M. Palma, R. Valderrama, M. Rodríguez-Ruiz, M. Chaki, L. A. del Río and J. B. Barroso, Immunological evidence for the presence of peroxiredoxin in pea leaf peroxisomes and response to oxidative stress conditions, *Acta Physiol. Plant.*, 2017, 39, 57.
- N. H. Cheng, J. K. Pittman, J. K. Zhu and K. D. Hirschi, The protein kinase SOS2 activates the Arabidopsis H⁺/Ca²⁺ antiporter CAX1 to integrate calcium transport and salt tolerance, *J. Biol. Chem.*, 2004, **279**, 2922–2926.
- 87 I. S. Day, V. S. Reddy, G. Shad Ali and A. S. Reddy, Analysis of EF-hand-containing proteins in *Arabidopsis.*, *Genome Biol.*, 2002, **3**, research0056.
- T. Z. Wang, J. L. Zhang, Q. Y. Tian, M. G. Zhao and W. H. Zhang, A *Medicago truncatula* EF-Hand family gene, *MtCaMP1*, is involved in drought and salt stress tolerance, *PLoS One*, 2013, **8**, e58952.

- H. Q. Zeng, Y. X. Zhang, X. J. Zhang, E. xu Pi and Y. Y. Zhu, Analysis of EF-hand proteins in soybean genome suggests their potential roles in environmental and nutritional stress signaling, *Front. Plant Sci.*, 2017, **8**, 887.
- 90 P. Rodziewicz, B. Swarcewicz, K. Chmielewska, A. Wojakowska and M. Stobiecki, Influence of abiotic stresses on plant proteome and metabolome changes, *Acta Physiol. Plant.*, 2014, 36, 1–19.
- V. Falara, T. A. Akhtar, T. T. H. Nguyen, E. A. Spyropoulou, P. M. Bleeker, I. Schauvinhold, Y. Matsuba, M. E. Bonini, A. L. Schilmiller, R. L. Last, R. C. Schuurink and E. Pichersky, The tomato terpene synthase gene family, *Plant Physiol.*, 2011, **157**, 770–789.
- 92 C. Q. Yang, X. M. Wu, J. X. Ruan, W. L. Hu, Y. B. Mao, X. Y. Chen and L. J. Wang, Isolation and characterization of terpene synthases in cotton (*Gossypium hirsutum*), *Phytochemistry*, 2013, **96**, 46–56.
- M. Valifard, S. Mohsenzadeh, B. Kholdebarin, V. Rowshan, A. Niazi and A. Moghadam, Effect of salt stress on terpenoid biosynthesis in *Salvia mirzayanii*: from gene to metabolite, *J. Hortic. Sci. Biotechnol.*, 2019, **94**, 389–399.
- 94 H. C. Zhou, L. F. Shamala, X. K. Yi, Z. Yan and S. Wei, Analysis of terpene synthase family genes in *Camellia sinensis* with an emphasis on abiotic stress conditions, *Sci. Rep.*, 2020, **10**, 933.
- 95 A. Baxter, R. Mittler and N. Suzuki, ROS as key players in plant stress signalling, J. Exp. Bot., 2014, 65, 1229–1240.

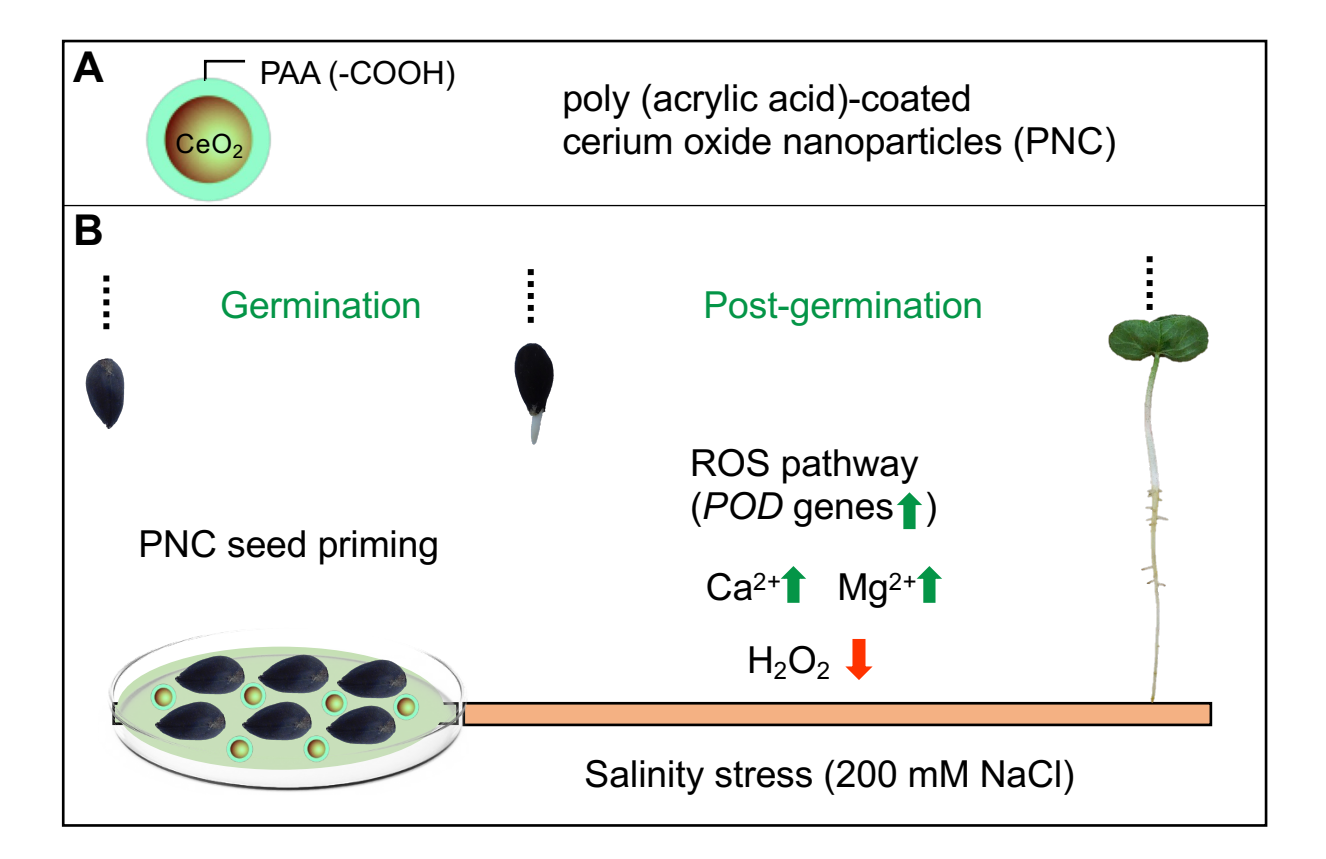


Figure 1. Influence of seed priming with cerium oxide nanoparticles (PNC) on cotton seedling development under salinity stress. Interfacing PNC with seeds (24 h) grown under salinity stress (200 mM NaCl) affects gene expression of reactive oxygen species (ROS) enzymatic pathways (e.g. peroxidase *POD* genes), Ca²⁺, and Mg²⁺ ion homeostasis. These molecular changes in seedling development improve root seedling development and tolerance to salt stress.

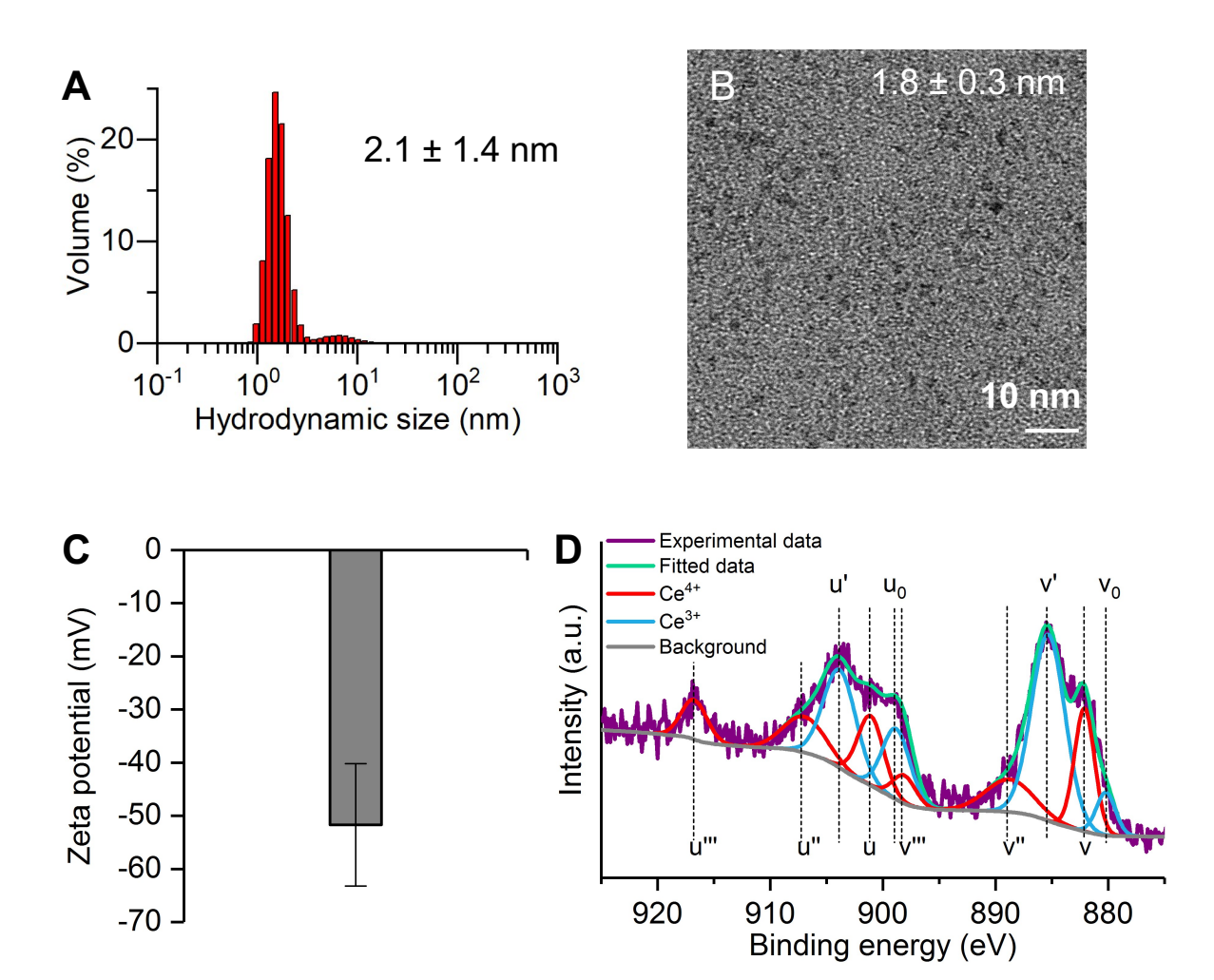


Figure 2. Characterization of cerium oxide nanoparticles (PNC). A, Hydrodynamic diameter measured by DLS in DI water (pH 8), B, representative TEM image, C, zeta potential, and D, XPS spectra showing Ce(III) = $u' + u_0 + v' + v_0$ and Ce(IV) = u''' + u'' + v''' + v'' + v. Error bar represents standard deviation, n = 3.

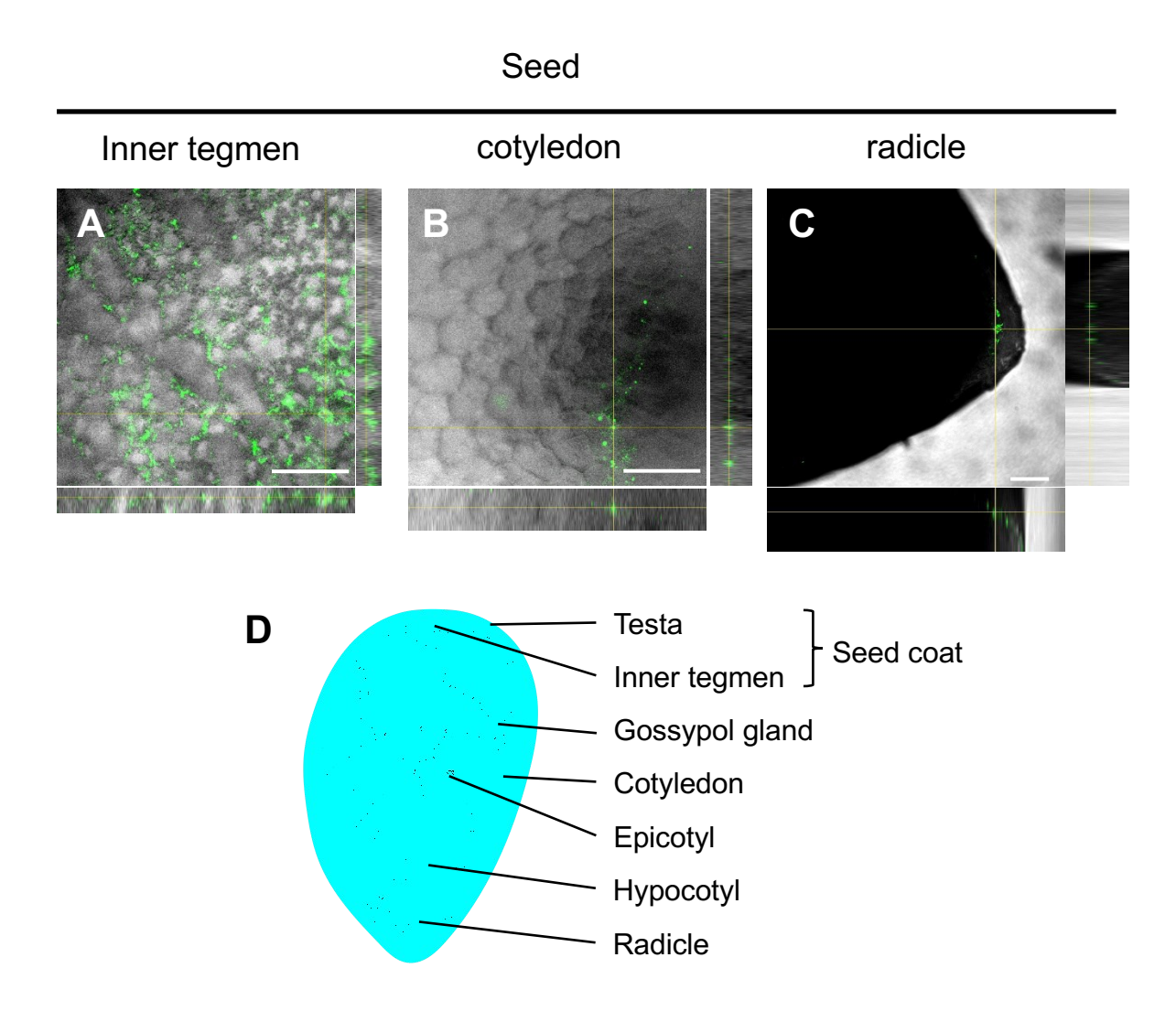


Figure 3. Cerium oxide nanoparticle (PNC) localization in cotton seed tissues. Confocal fluorescence microscopy images after 24 h of seed priming with PNC labeled with the fluorescent dye Dil (green). The nanoparticles were localized in the $\bf A$, seed coat within the inner tegmen, $\bf B$, in cotyledons, and $\bf C$, the radicle. Scale bar = 50 μ m. $\bf D$, Schematic diagram of cotton seed structure.

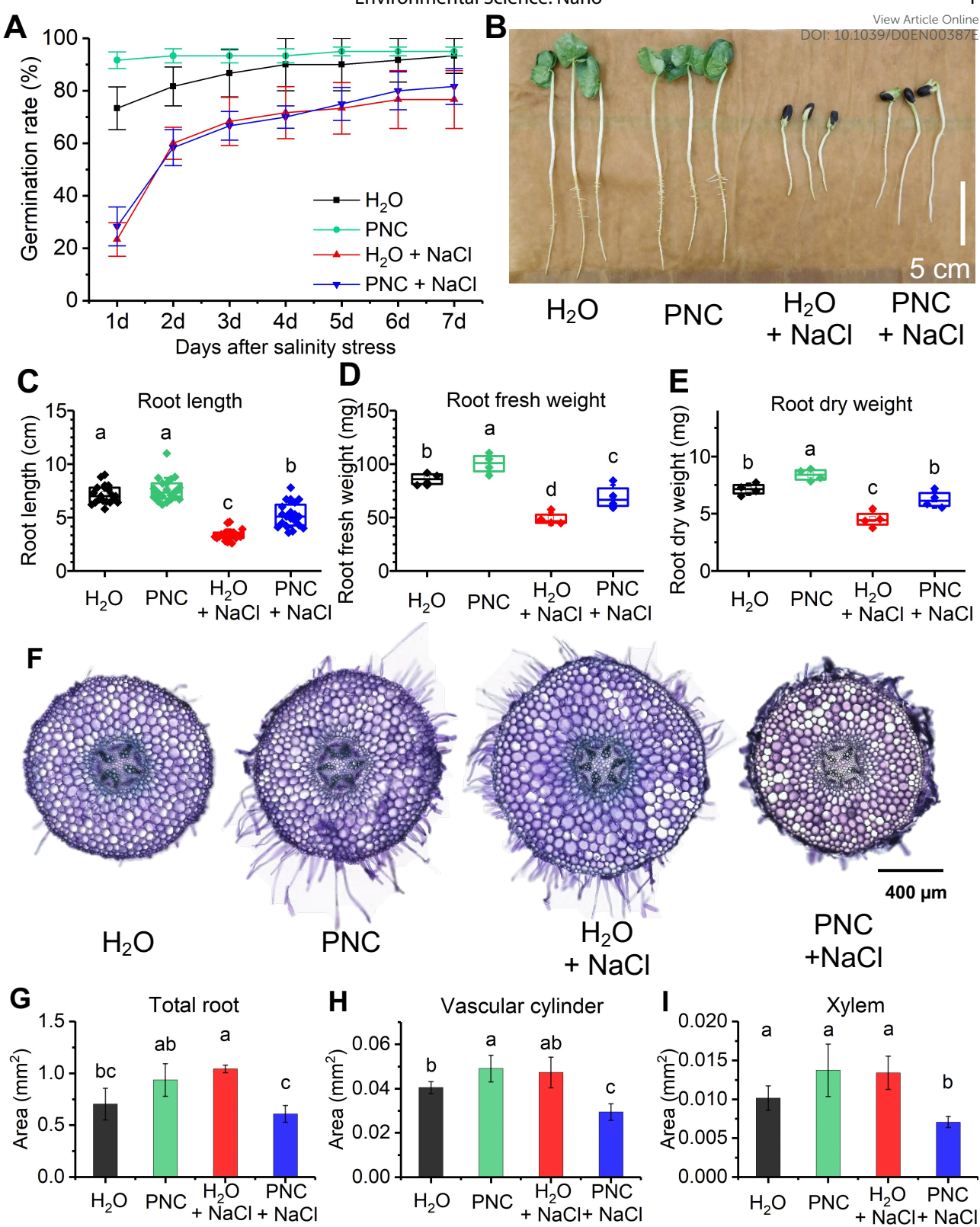


Figure 4. Modification of seedling root development under salinity stress by cerium oxide nanoparticles (PNC). A, PNC do not impact seed germination rates under salinity stress (200 mM NaCl). B, PNC modify root development by enhancing root \mathbf{C} , length, \mathbf{D} , fresh weight, and \mathbf{E} , dry weight, as shown with box plots. \mathbf{F} , Representative cross sections of cotton roots stained with toluidine blue. The changes in root morphology and biomass are accompanied by reductions in \mathbf{G} , root cross sectional area, \mathbf{H} , vascular cylinder and \mathbf{I} , xylem area. Boxes represent the interquartile range from the first to the third quartile with squares as the medians. Statistical comparisons were performed by independent samples one-way ANOVA on Duncan's test (two tailed) or Kruskal Wallis test. Data with different lowercase letter indicate significant differences (P < 0.05). Error bars indicate standard deviation, $n \ge 4$.

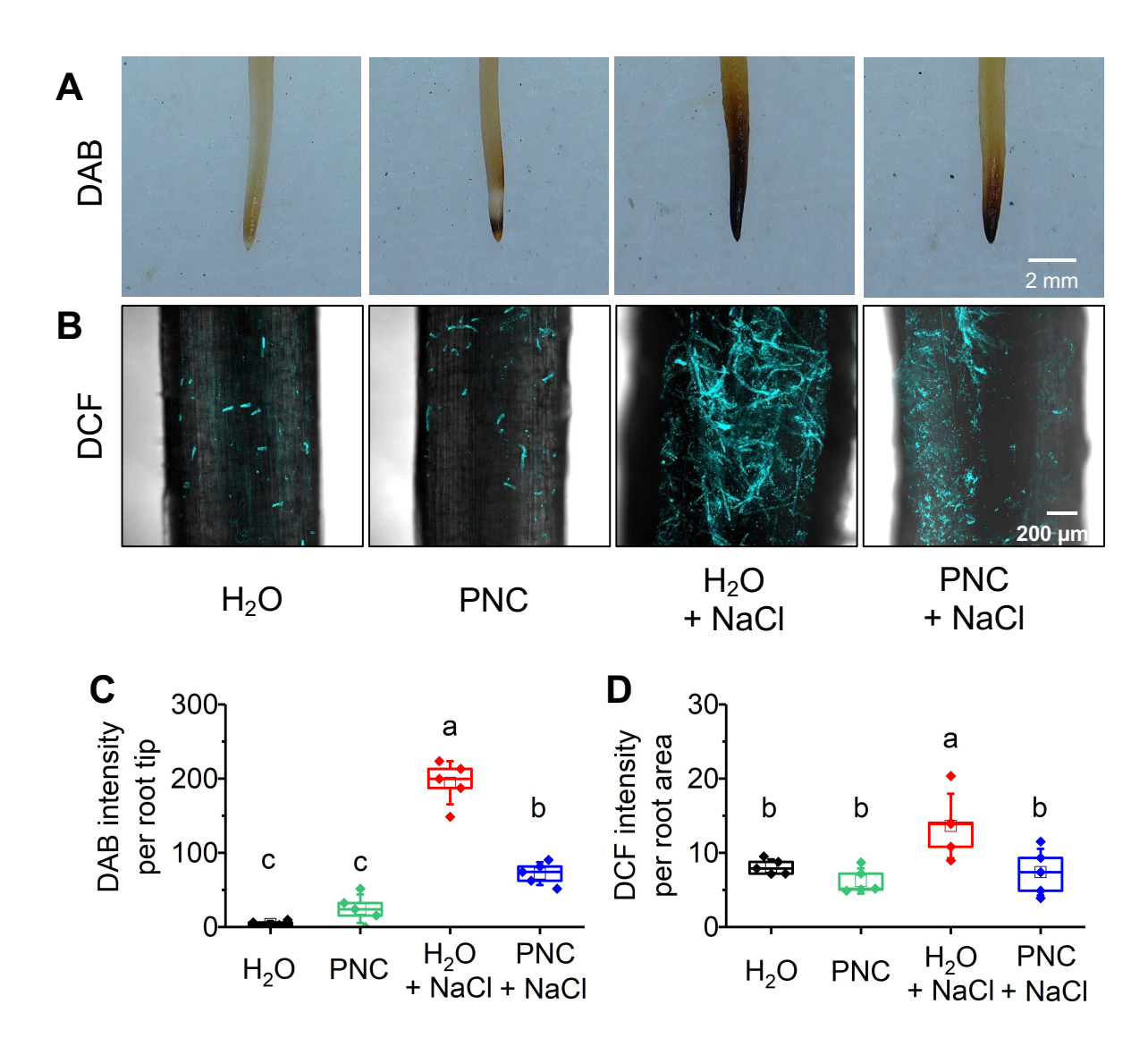


Figure 5. ROS scavenging by cerium oxide nanoparticles (PNC) in cotton seedling roots under salinity stress. A, Representative DAB staining images reflecting hydrogen peroxide levels in cotton seedling root tips. B, Confocal microscopy images of DCF fluorescent dye indicating ROS levels in cotton seedling root maturation zone. Quantitative analysis of \mathbf{C} , DAB staining intensities in cotton root tip and \mathbf{D} , area normalized DCF intensity in cotton root maturation zone. Boxes represent the interquartile range from the first to the third quartile with squares as the medians. Statistical comparisons were performed by independent samples one-way ANOVA on Duncan's test (two tailed). Data with different lowercase letters indicate significant differences (P < 0.05). Error bars indicate standard deviation, n = 5.

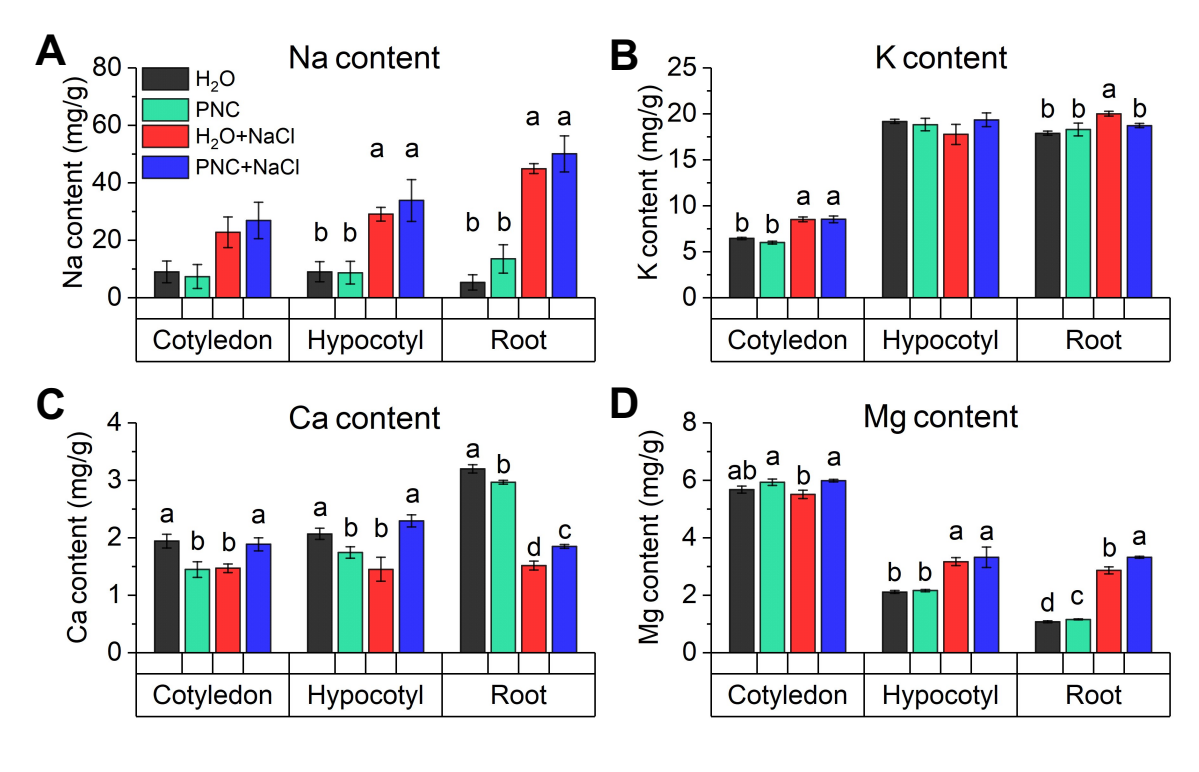


Figure 6. Effect of cerium oxide nanoparticles (PNC) on ion content in cotton seedlings exposed to salt stress. Concentration of A, Na, B, K, C, Ca, and D, Mg in cotton seedling cotyledons, hypocotyls and roots. Ion content levels were measured by ICP-OES. Statistical comparisons were performed by independent samples one-way ANOVA on Duncan's test (two tailed) or Kruskal Wallis test. Data with different lowercase letters indicate significant differences (P < 0.05). Error bars indicate standard error, $n \ge 3$.

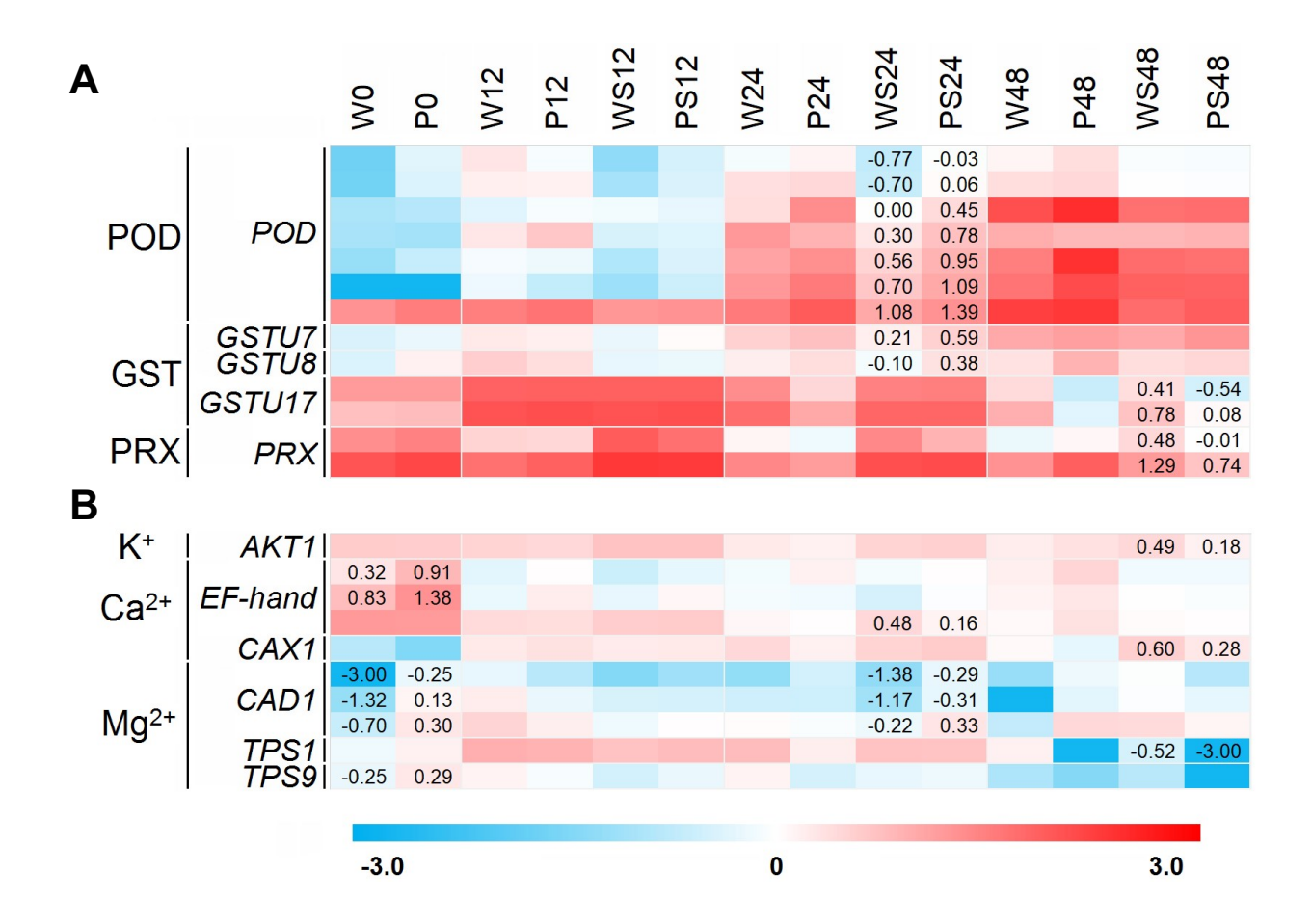


Figure 7. Expression profiling of genes related to ion homeostasis and ROS pathway. Heat maps showing the expression level ($\log_{10}(\text{FPKM} + 0.001)$), FPKM, fragments per kilobase of exon model per million mapped reads) of differentially expressed genes (DEG). Numbers are indicated at time points when the transcript expression level between PNC priming and water control was significantly different (n = 3, adjusted *P*-value < 0.05 and fold change \geq 1). RNA-seq analysis of genes associated with **A**, ROS related enzymes POD, GST, and PRX, **B**, K⁺, Ca²⁺, and Mg²⁺ homeostasis. W0: after H₂O priming and before salinity stress. P0: after PNC priming and before salinity stress. W12, W24, W48: after H₂O priming and grown under normal conditions for 12, 24 and 48 h, respectively. P12, P24, P48: after PNC priming and grown under salinity stress for 12, 24 and 48 h, respectively. PS12, PS24, PS48: after PNC priming and grown under salinity stress for 12, 24 and 48 h, respectively. PS12, PS24, PS48: after PNC priming and grown under salinity stress for 12, 24 and 48 h, respectively.

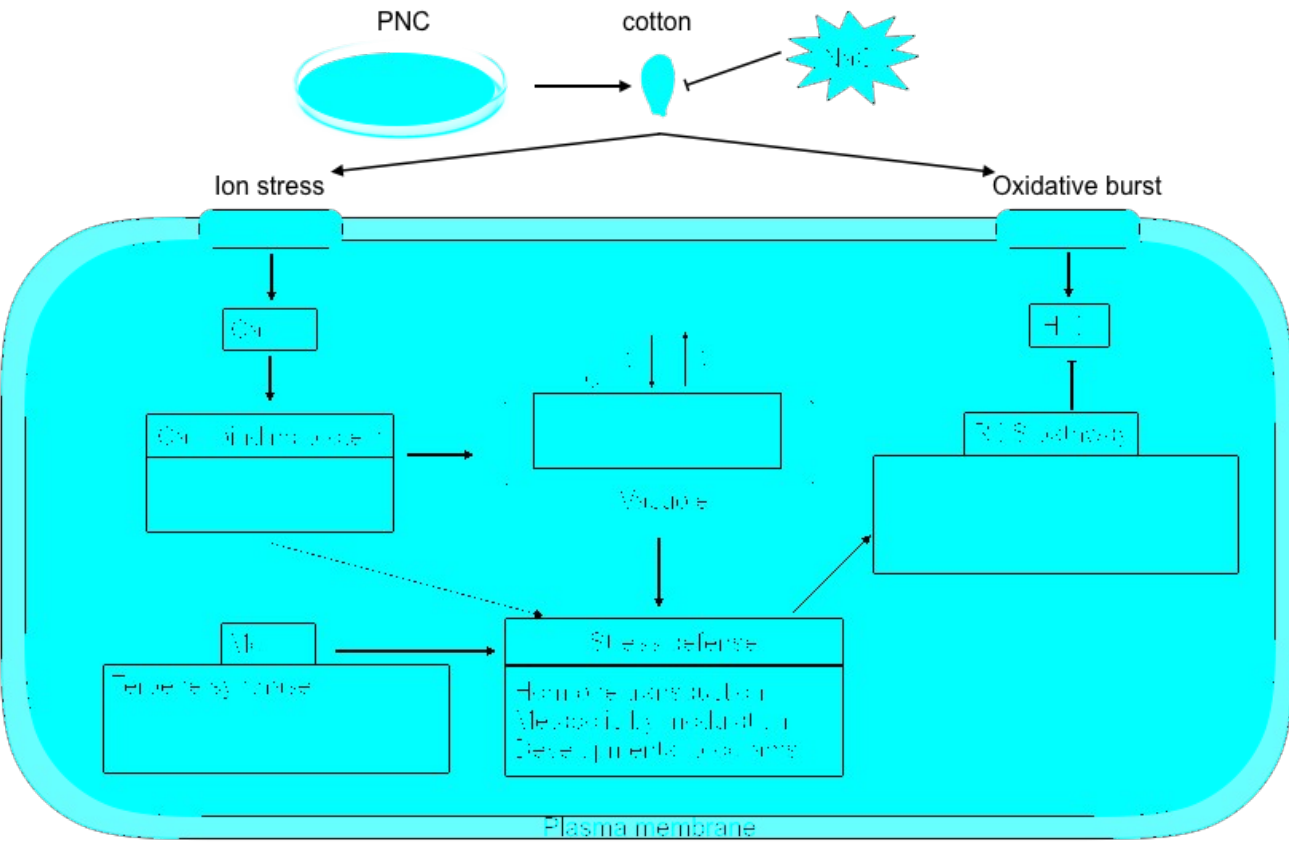


Figure 8. Molecular interaction network of how cerium oxide nanoparticles (PNC) impact cotton seedling development under salinity stress. Salinity stress induce ion stress and oxidative burst, increase the H₂O₂ in plant cell. PNC priming influences ion homeostasis (Ca²⁺, and Mg²⁺), boosts the ROS pathway, and stress defense response that results in improved cotton seedling salinity tolerance. Up-regulated genes (green with upward-pointing arrows) and down-regulated genes (red with downward-pointing arrows) at a given time point.

TOC

